

Particle-antiparticle oscillation modes crossing horizon: baryogenesis and dark-matter waves

She-Sheng Xue

ICRANet Piazzale della Repubblica, 10 -65122, Pescara, Italy
Physics Department, Sapienza University of Rome, Rome, Italy
INFN, Sezione di Perugia, Perugia, Italy
ICTP-AP, University of Chinese Academy of Sciences, Beijing, China

E-mail: xue@icra.it and she-sheng.xue@cern.ch

Abstract. Quantum massive particle and antiparticle pair production and oscillation during reheating result in a holographic and massive pair plasma state. Perturbations in the densities of particles and antiparticles within this plasma form acoustic waves, characterized by symmetric and asymmetric density contrasts. By deriving the acoustic wave equations and identifying the frequencies of the lowest-lying perturbation modes (with zero wave number), the study shows that the wavelengths of these modes, when compared with the horizon size, suggest the possibility of superhorizon crossing during reheating. This crossing leads to particle-antiparticle asymmetry observable by an observer inside the horizon. The decay of massive particles and antiparticles into baryons generates a net baryon number, potentially explaining baryogenesis. The calculated baryon number-to-entropy ratio aligns with observational data. This crossing also accounts for dark matter particle-antiparticle asymmetry in the present Universe. The study also explores perturbation modes with nonzero wave numbers, representing dark-matter acoustic waves. These modes exited the horizon and re-entered after recombination, potentially imprinting on the matter power spectrum at large length scales and influencing the formation of large-scale structures and galaxies.

Contents

1	Introduction	2
2	A brief review of $\tilde{\Lambda}$CDM applied to inflation and reheating	4
3	Particle and antiparticle density perturbations	9
3.1	Equations for particle and antiparticle density perturbations	9
3.1.1	Continuity and Eulerian equations	10
3.1.2	Contrast density perturbations	11
3.2	Equations for symmetric and asymmetric density perturbations	12
3.2.1	Acoustic wave equations	12
3.2.2	Lowest-lying mode oscillating equations	13
3.2.3	Particle-antiparticle asymmetry due to modes' horizon crossing	14
4	Particle-antiparticle oscillation and horizon crossing	17
4.1	Under- and over-damped oscillating modes	17
4.2	Lowest-lying oscillation mode crossing horizon	18
5	Oscillating amplitudes at horizon crossing	19
5.1	Lowest-lying mode amplitudes at horizon crossing	20
5.2	Particle-antiparticle asymmetry due to horizon crossing	20
6	Subhorizon crossing in pre-reheating	21
6.1	Particle-antiparticle asymmetry in pre-inflation and inflation	21
6.2	Particle-antiparticle symmetry in massive pair episode	22
6.3	Subhorizon crossing point in pre-reheating episode	23
7	Superhorizon crossing in genuine reheating	24
7.1	Superhorizon crossing point in massive pair episode	24
7.2	Particle-antiparticle asymmetry occurs in reheating epoch	25
8	Baryogenesis in reheating epoch	27
8.1	Initial baryon asymmetry for standard cosmology	27
8.2	Net baryon numbers and baryon number-to-entropy ratio	27
9	Dark-matter acoustic wave and large-scale structure	29
9.1	Wave modes, horizon crossings, and Jeans instability	30
9.1.1	Subhorizon stable modes and dark-matter acoustic waves	31
9.1.2	Unstable superhorizon modes and large-scale structure	32
9.2	Particle-antiparticle “neutral plasma” acoustic wave	33
10	Summary and remarks	35

1 Introduction

In modern cosmology, as described by the Λ cold dark matter model (Λ CDM), several long-standing issues persist, including the cosmological constant Λ (dark energy), inflation, reheating, dark matter, and the coincidence and fine-tuning problems. Inflation [1–7] and reheating [8–17] are fundamental epochs leading to the hot Big Bang of standard cosmology. Massive particle production and decay play crucial roles in ending inflation and initiating reheating. Numerous studies [18–26] focus on the spontaneous gravitational creation of massive particle X and antiparticle \bar{X} pairs in the early Universe. These particles have masses M larger than the horizon scale H . Some of these particles are stable and could be candidates for massive dark matter particles, while others are unstable and decay into Standard Model (SM) particles and/or less massive dark-matter particles. These massive particles X and antiparticles \bar{X} are gravitationally created in pairs, persevering the CPT (charge-parity-time) particle-antiparticle symmetry with equal numbers of particles and antiparticles, resulting in a net particle number is zero.

The inflation would erase any initial particle-antiparticle asymmetry. During reheating, some massive particle-antiparticle pairs annihilate into SM particles, contributing the leptons and baryons content and increasing entropy. After reheating, the Universe evolves adiabatically with conserved entropy. All processes preserve the fundamental CPT symmetry of particles and antiparticles. Therefore, the observation of the baryon and anti-baryon asymmetry, i.e., the baryon number-to-entropy ratio $n_B/s = 0.864^{+0.016}_{-0.015} \times 10^{-10}$ [27], demands an explanation for the baryon asymmetry of the universe, necessitating an understanding of baryogenesis.

In the context of particle physics and cosmology, the absence of initial particle-antiparticle asymmetry leads to the conclusion that the problem of baryon asymmetry requires a dynamic solution characterized by three necessary conditions [28]:

- (i) Baryon number B and lepton number L non-conservation processes are sources for producing baryon and lepton numbers. For instance, in the Grand Unified Theory, particles X decay processes such as $X \rightarrow Y + B(L)$ contribute to this production. Additionally, the violation of the $B + L$ number by the instanton and sphaleron vacuum structure of the SM in particle physics also plays a role;
- (ii) C-symmetry and CP-symmetry violations avoid the \bar{X} antiparticle processes $\bar{X} \rightarrow \bar{Y} + \bar{B}(\bar{L})$ of producing anti-baryon(lepton) number. Namely, if particles X and antiparticles \bar{X} have the same numbers, they must have different decay rates due to CP-symmetry violations. The complex phase of SM fermion families mixing explicitly breaks the CP-symmetry, as shown in the neutral K and B systems. The CP asymmetry can also be generated by spontaneous symmetry breaking.
- (iii) The system should depart from thermal equilibrium. It occurs when microscopic interaction rates are smaller than the macroscopic evolution rate. Otherwise, the process $X \rightarrow Y + B(\bar{L})$ would be compensated by the inverse process $Y + B(\bar{L}) \rightarrow X$ and therefore the total net baryon number remains zero.

We recall that these Sakharov conditions are satisfied in the standard cosmology model and the SM of particle physics. However, the effect on baryogenesis is insufficient to match the observed baryon number-to-entropy ratio. Particle physicists have proposed numerous ideas to explain baryon asymmetry, incorporating elements beyond the SM [29–32]. One notable approach is the dynamic process of electroweak baryogenesis, which involves the first-order phase transition of electroweak symmetry breaking of the SM nontrivial vacuum [33, 34]. In addition, several studies have explored intriguing connections between reheating and baryogenesis [35–46].

In this article, we do not consider an alternative dynamic solution for baryogenesis following the Sakharov conditions by introducing explicit or spontaneous breaking of the CPT symmetry of particles and antiparticles in Lagrangian or ground state in the Universe evolution. Instead, we attempt to explain baryogenesis by studying the horizon-crossing dynamics that possibly cause the different number between massive particles X and antiparticles \bar{X} pairs, which are equally produced in the reheating epoch. Such a difference provided an initial value of particle and antiparticle asymmetry that preserves the entire Universe after the reheating, possibly accounting for baryogenesis and dark matter particle and antiparticle asymmetry. We briefly describe the horizon-crossing dynamics below, and detailed discussions and equations will be in the main text.

In conjunction with the rapidly oscillating component H_{fast} of the horizon, the production and oscillation of particle X and antiparticle \bar{X} pairs maintains the fundamental CPT symmetry. It does not produce different numbers of particles and antiparticles, i.e., particle and antiparticle asymmetry. However, these X particles and \bar{X} antiparticles undergo pair oscillations with each other, and their local and instantaneous distributions (densities) are different (not in phase) in spacetime. Moreover, the pair oscillation frequency or wavelength depends on the horizon evolution in reheating. As a consequence, two possible situations can occur.

First, if the wavelength of pair oscillating modes is smaller than the horizon size. The local difference of particle and antiparticle distributions (densities) would tend to average to zero across different patches inside the horizon. All particles and antiparticles are inside the horizon, and particle and antiparticle asymmetry does not occur. Second, if pair oscillating modes cross out the horizon when their wavelength exceeds the size of the horizon. In other words, such super-horizon crossing occurs when the horizon expansion rate is smaller than the oscillating frequency of particle and antiparticle modes. Such super-horizon modes freeze outside the horizon and never return to the horizon. Consequently, the local difference in particle and antiparticle distributions (densities) would not tend to average to zero across different patches inside the horizon. The different numbers of particles and antiparticles appear inside the horizon, resulting in a net X and \bar{X} particle number, namely the particle and antiparticle asymmetry for observers inside the horizon. In both situations, the total sum of X and \bar{X} particle numbers inside and outside the horizon remains zero, as required by particle number conservation during their production and oscillation.

Moreover, through massive particles (pairs) decay (annihilate) to SM particles within the horizon, such an $X - \bar{X}$ asymmetry in the reheating could be an initial

source for the asymmetry between SM particles and antiparticles, namely the lepton and baryon numbers $B + L$ violation while conserving $B - L$ and electric charge in the present Universe.

We will investigate the horizon-crossing dynamics and phenomena potentially responsible for producing the initial particle and antiparticle asymmetry inside the horizon during the reheating epoch and how this relates to the observed baryogenesis. Notably, the horizon-crossing dynamics and phenomena are analogous to the super-horizon crossing of curvature perturbation modes during the inflation epoch, where they freeze outside the horizon and later reenter the horizon, influencing the formation of large-scale structures. The article is organized as follows. In Sec. 2, we briefly review the X particles and \bar{X} antiparticle productions and oscillations, and their dynamics effects on inflation [47], reheating [48] and standard cosmology [49] in the $\tilde{\Lambda}$ CDM model. Section 3 describes the particle-antiparticle symmetric and asymmetric contrast density perturbations and derives their acoustic wave equations. In Sec. 4, we analyze the wavelengths of acoustic modes. In Secs. 5, 6 and 7 we discuss horizon crossings that result in particle and antiparticle asymmetry. Consequently, we calculate the baryon number-to-entropy ratio in Section 8. Additionally, building on preliminary studies of dark matter waves [47], Section 9 examines dark-matter acoustic waves for a given comoving wavelength and their relevance to physical observations and effects at large-distance scales. In this article, $G = M_{\text{pl}}^{-2}$ is denoted as the Newton constant, where M_{pl} is the Planck scale. The reduced Planck scale $m_{\text{pl}} \equiv (8\pi)^{-1/2} M_{\text{pl}} = 2.43 \times 10^{18} \text{GeV}$.

2 A brief review of $\tilde{\Lambda}$ CDM applied to inflation and reheating

In the framework of the recently proposed $\tilde{\Lambda}$ CDM ($\tilde{\Lambda}$ cold dark matter) scenario, we study dynamics and phenomena of inflation [47], reheating [48] and standard cosmology [49] in accordance with observations. For the convenience of readers, we begin with a brief review of the main features of the $\tilde{\Lambda}$ CDM scenario.

First, we propose a time-varying cosmological $\tilde{\Lambda}(t)$ term in the Friedman equation, representing dark energy interacting with matter and radiation. The Friedman equations for a flat Universe of horizon H are [50]

$$H^2 = \frac{8\pi G}{3}\rho; \quad \dot{H} = -\frac{8\pi G}{2}(\rho + p), \quad (2.1)$$

where energy density $\rho \equiv \rho_M + \rho_R + \rho_\Lambda$ and pressure $p \equiv p_M + p_R + p_\Lambda$. The equations of state are $p_{M,R,\Lambda} = \omega_{M,R,\Lambda}\rho_{M,R,\Lambda}$, $\omega_M = 0$, $\omega_R = 1/3$ and $\omega_\Lambda = -1$ for matter ρ_M , radiation ρ_R and dark energy ρ_Λ densities respectively.

The second equation of (2.1) represents the generalized conservation law (Bianchi identity) for a time-varying cosmological term (dark energy) $\rho_\Lambda(t) \equiv \tilde{\Lambda}/(8\pi G)$, as it interacts with matter/radiation $\rho_{M,R}$. It reduces to the usual equation $\dot{\rho}_{M,R} + (1 + \omega_{M,R})H\rho_{M,R} = 0$ and $\dot{\rho}_\Lambda = 0$ when non-interacting ρ_Λ is constant in time. Future research will be on the microscopic origin and nature of the cosmological term and its interaction with matter.

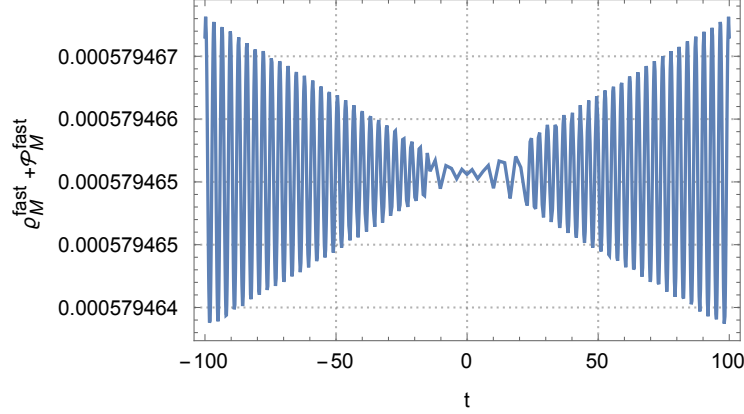


Figure 1. We reproduce the Fig. 1 of Ref. [48] to illustrate the coherent quantum oscillations on the state $|\mathcal{N}_{\text{pair}}\rangle$, which are back-and-forth production and annihilation of massive particle and antiparticle pairs in microscopic space and time t in the unit of the characteristic time scale M^{-1} of quantum processes. It is described by quantum pair energy density ρ_M^{fast} and pressure $\mathcal{P}_M^{\text{fast}}$ (momentum density) in the unit of $\rho_{\text{crit}} = 3m_{\text{pl}}^2 H_{\text{slow}}^2$, and the relevant dynamics equations are in Ref. [48]. When the time $t \gg 1/M$, pair coherent oscillations approach the equilibrium configuration described by a massive pair plasma fluid (2.2).

Second, the massive particle-antiparticle pairs production [18] and oscillation [47, 48] establish a condensate ground state $|\mathcal{N}_{\text{pair}}\rangle$ characterized by the large number ($\mathcal{N}_{\text{pair}} \gg 1$) of massive ($M \gg H$) pairs. These pairs are attributed to the microscopic fast-component H_{fast} in the Hubble function $H = H_{\text{fast}} + H_{\text{slow}}$. The fast component H_{fast} oscillates coherently with massive pairs’ quantum oscillation, which is related to the production, kinematic motion and annihilation of massive pairs at the “microscopic” spacetime scale $1/M$, as illustrated in Fig. 1. Massive particles and antiparticles are produced along with their kinetic energy and oscillate with H_{fast} in space and time due to their nonlinear interaction. These pair oscillations (fluctuations) imply that particles and antiparticles’ local and instantaneous distributions (densities) are not identically in phase in space and time. However, particle and antiparticle symmetry conserves for the total particle and antiparticle numbers are the same. It is analogous to the dynamics and phenomena of creation and oscillation of electrons and positrons along with strong electric fields [51–53].

The local and fast-oscillating H_{fast} dynamics behaviours are consistent with recent studies of vacuum fluctuation and “microcyclic universes” at small scales, demonstrated by local scale factor oscillation, as shown in Figure 1 of Refs. [54, 55]. The slow component H_{slow} obeys the Friedman equation (2.1) at the “macroscopic” time scale $1/H$. The functional amplitude H_{slow} is much larger than H_{fast} with $H_{\text{slow}} \approx H$, and subsequently, we will drop the subscript “slow” henceforth.

These “microscopic” and “macroscopic” processes are non-linearly coupled. One has difficulties even numerically integrating coupled differential equations simultaneously due to the vast difference between the scales $1/M$ and $1/H$. Therefore, we have to model the condensate state $|\mathcal{N}_{\text{pair}}\rangle$ as a macroscopic “equilibrium” or “equipartition” plasma fluid state by averaging the fast component H_{fast} and pairs’ oscillations

(Fig. 1) over microscopic time and length scales. This method allows us to study the back-reactions of fast component H_{fast} and pairs' oscillation state $|\mathcal{N}_{\text{pair}}\rangle$ on the Friedman equation (2.1). More detailed discussions are in Secs. 2-3, Figure 1 and Appendix “Quantum pair oscillation details” of Ref. [48].

Third, we describe this “equilibrium” plasma fluid state as a perfect fluid state characterized by the effective number density n_M^H and energy density ρ_M^H of massive stable and unstable pairs of particles X and antiparticles \bar{X} ,

$$\rho_M^H \equiv 2\chi m^2 H^2, \quad n_M^H \equiv \chi m H^2, \quad (2.2)$$

the pressure and equation of state are $p_M^H = \omega_M^H \rho_M^H$. Here, m is the effective mass parameter representing the total mass and number of pairs in the massive pair plasma state. The lower limit $\omega_M^H \approx 0$ for $m \gg H$ characterizes a non-relativistic massive plasma fluid in reheating [48], which is relevant for the study in this article. Whereas, the upper limit $\omega_M^H \lesssim 1/3$ for $m \gtrsim H$ is relevant for studying inflation [47].

Particle and antiparticle pair oscillations in spacetime establish the equilibrium state (2.2) when the time $t \gg 1/M$. This massive plasma fluid state is a holographic layer near the horizon because pair-oscillation contributions cancel each other from different patches inside the horizon. The spatial average of local pairs' and H_{fast} oscillations over the length scale $1/M$ vanish *inside* the horizon. The quantum oscillations of massive particle and antiparticle pairs' production, kinematic motion and annihilation occur near the horizon. We use the effective width parameter χ to characterize the layer radial width $\lambda_m = (\chi m)^{-1} \ll H^{-1}$. We will adopt ¹ $\chi = 10^{-3}$ and treat m as a free parameter, whose value depends on the Universe's evolution epoch. Thus, at a given horizon H , the “macroscopic” condensation state of pair plasma fluid ρ_M^H (2.2) effectively represents the average overall “microscopic” states of the fast component H_{fast} , pair production and oscillations at the time and length scale $1/M$. More detailed discussions are in Sec. 3-4 of Ref. [48].

Fourth, we need to take into account how the horizon H variation governed by the Freeman equations (2.1) back-reacts on the equilibrium state (2.2), in other words, how the equilibrium state responds to the H variation. For this reason, we propose the cosmic rate equation (2.5) to describe the interaction between the massive pair plasma energy density ρ_M^H (2.2) and normal matter density ρ_M in Freeman equation (2.1), because their time scales of responding H variation are very different. The normal matter density ρ_M time scale is $\tau_H \approx H^{-1}$. While, the massive pair plasma energy density ρ_M^H time scale τ_M responding the H variation can be estimated as follows,

$$\tau_M^{-1} = \Gamma_M, \quad \Gamma_M = \frac{dN}{2\pi dt} \approx \frac{\chi m}{4\pi} \epsilon, \quad (2.3)$$

where $N \approx n_M^H H^{-3}/2$ is the pairs' number inside the Hubble sphere (averaged over volume) and Γ_M is the rate of pair production and oscillation affected by the horizon

¹In previous studies [56, 57], a renormalization prescription at high energies $M \gg H$, which is different from the usual prescription (subtraction) at low energies $M \ll H$, consistently yields the mean density $n_M^H \approx \chi m H^2$ (2.2) and effective width parameter $\chi \approx 1.85 \times 10^{-3}$ by examining massive fermion pair productions in an exact De Sitter spacetime of constant H and scaling factor $a(t) = e^{iHt}$. This result suggests $\chi \sim \mathcal{O}(10^{-3})$

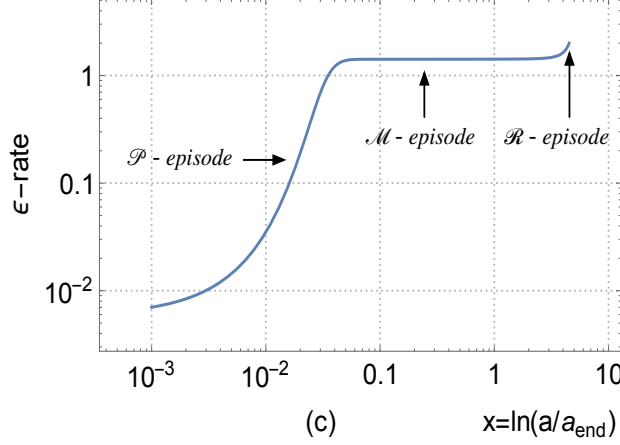


Figure 2. (Color Online). In a few e -folding number $x = \ln(a/a_{\text{end}})$ during the reheating epoch, the H -variation ϵ -rate (2.4) indicates three distinct episodes: (i) $\epsilon < 1$ pre-reheating episode (\mathcal{P} -episode) of massive pairs production, (ii) $\epsilon \approx 3/2$ massive pair oscillation domination episode (\mathcal{M} -episode), and (iii) $\epsilon \approx 2$ radiation domination episode (\mathcal{R} -episode) of genuine reheating due to massive pairs decaying into relativistic particles. The \mathcal{P} -episode is much shorter than \mathcal{M} - and \mathcal{R} -episodes. The a_{end} indicates when the inflation ends $H \approx \Gamma_M$. The pre-inflation and inflation are in the regime $x = \ln(a/a_{\text{end}}) < 0$, where $H > \Gamma_M$ and $\epsilon \ll 1$, when dark-energy $\tilde{\Lambda}$ dominates. We reproduce this figure from Fig. 6 (c) of Ref. [48]. The relevant dynamical equations are (2.1), (2.5) and (2.6). The time scale H^{-1} governs this process, and time scale $\tau_M = \Gamma_M^{-1}$ plays its role at the first turning point from \mathcal{P} to \mathcal{M} , and $\tau_R = (\Gamma_M^{\text{de}})^{-1}$ plays its role at the second turning point from \mathcal{M} to \mathcal{R} . Note that in the \mathcal{M} - and \mathcal{R} -episodes, the evolution rate $\epsilon \approx 3/2, 2$ (2.4) and the relaxation rate $\Gamma_M \propto \epsilon$ (2.3) are approximately constant in time.

H change in time, governed by the Friedman equation (2.1). We consider the τ_M is a relaxation time of pair plasma fluid (2.2) responding to the H variation. This shows that the rate Γ_M relates to the pair plasma fluid energy density ρ_M^H interaction with other energy density components $\rho_{R,M,\Lambda}$ in the Friedman equation (2.1). The time scale τ_M is significantly larger than the microscopic time scale $1/M$ for pairs' quantum oscillations (Fig. 1) but smaller than the macroscopic time scale $1/H$ of $\rho_{R,M,\Lambda}$ density variation. It effectively describes the “relaxation” time scale, indicating how the massive pair plasma state varies in response to the macroscopic time as the Universe horizon $H(\rho_M, \rho_R, \rho_\Lambda)$ evolves. The Universe evolution ϵ -rate is usually defined as,

$$\epsilon \equiv -\frac{\dot{H}}{H^2} = \frac{3}{2} \frac{(1 + \omega_M)\rho_M + (1 + \omega_R)\rho_R}{\rho_\Lambda + \rho_M + \rho_R}. \quad (2.4)$$

The second equation arises from the Friedman equations (2.1). The asymptotic values $\epsilon \ll 1$, $\epsilon \approx 2$ and $\epsilon \approx 3/2$ correspond to dark energy, radiation, and matter domination, respectively. Fig. 2 shows the ϵ variation in the reheating, indicating the nonlinear behaviour of the crucial quantity $\Gamma_M \propto \epsilon$ (2.3) adopted for the analyses of this article.

The massive pair plasma state density ρ_M^H (2.2), associated with the horizon, contributes to the normal matter/radiation density $\rho_{M,R}$. In turn, the $\rho_{M,R}$ variation

affects the ρ_M^H via the horizon H . This interaction implies a non-linear back-and-forth interplay between the massive pair plasma state and the matter state during the Universe's evolution. Moreover, the massive pair plasma state has a microscopic “relaxation” time scale τ_M (2.3), differing from the macroscopic one $\tau_H \approx H^{-1}$ of the matter and radiation state $\rho_{M,R}$ in the Friedman equation (2.1), i.e., $\tau_H \gg \tau_M$. Therefore, we cannot simply add ρ_M^H into $\rho_{M,R}$ in the Friedman equation.

By analogy with the Boltzmann rate equation for a microscopic back-and-forth process, e.g., $e^+e^- \Leftrightarrow \gamma\gamma$, in the macroscopic hydrodynamical expansion (see part of Eq. (5.4) in Ref. [48]), we propose the back-and-forth interaction between the densities ρ_M^H and $\rho_{M,R}$ follows the cosmic rate equations of Boltzmann type,

$$\dot{\rho}_M + 3(1 + \omega_M)H\rho_M = \Gamma_M(\rho_M^H - \rho_M - \rho_R) - \Gamma_M^{\text{de}}\rho_M^{\text{de}}, \quad (2.5)$$

$$\dot{\rho}_R + 3(1 + \omega_R)H\rho_R = \Gamma_M(\rho_M^H - \rho_M - \rho_R) + \Gamma_M^{\text{de}}\rho_M^{\text{de}}. \quad (2.6)$$

The term $3(1 + \omega_{M,R})H\rho_{M,R}$ with the time scale $[3(1 + \omega_{M,R})H]^{-1}$ represents the space-time expanding effect on the density $\rho_{M,R}$. The detailed balance term $\Gamma_M(\rho_M^H - \rho_M - \rho_R)$ indicates how densities ρ_M^H and $\rho_{M,R}$ of different time scales couple together in back-and-forth interaction. $\Gamma_M\rho_M^H$ is the source term, indicating ρ_M^H contribution to increasing $\rho_{M,R}$. $\Gamma_M\rho_{M,R}$ is the depletion term, indicating back reaction reducing $\rho_{M,R}$. The ratio $\Gamma_M/H > 1$ indicates the coupled case, and $\Gamma_M/H < 1$ indicates the decoupled case.

There are unstable massive pairs of density ρ_M^{de} inside the massive pair plasma state (2.2). The term $-\Gamma_M^{\text{de}}\rho_M^{\text{de}}$ in (2.5) represents unstable massive pairs decay to SM particles and other sterile dark-matter particles, whose masses are much smaller than massive pairs. They are ultra-relativistic particles (radiation) in the reheating epoch, described by the cosmic rate equation (2.6) with the term $+\Gamma_M^{\text{de}}\rho_M^{\text{de}}$ for energy conservation. The decay rate is $\Gamma_M^{\text{de}} \approx g_Y^2 \hat{m}$ and time scale is $\tau_R = (\Gamma_M^{\text{de}})^{-1}$, where g_Y is the Yukawa coupling between massive pairs and relativistic particles. In the reheating epoch, we adopt the mass parameter $m = \hat{m} = 27.7m_{\text{pl}}$ and $g_Y^2 = 10^{-9}$ [48]. The cosmic rate equation (2.6) for relativistic particles reduces to the usual reheating equation [58] when $\Gamma_M^{\text{de}} \gg \Gamma_M$. Actually, the scale $\tau_R = (\Gamma_M^{\text{de}})^{-1}$ is the reheating time scale. The detailed discussions are in Secs. 4-5 of Ref. [48].

To explicitly show the interaction between dark energy and matter, we can use the cosmic rate equations (2.5) and (2.6) to recast the Friedman equations (2.1) as a dark-energy equation

$$\dot{\rho}_\Lambda + 3(1 + \omega_\Lambda)H\rho_\Lambda = -2\Gamma_M(\rho_M^H - \rho_M - \rho_R), \quad (2.7)$$

where $\Gamma_M(\rho_M^H - \rho_M - \rho_R)$ represents the interaction between dark energy and matter/radiation via the massive pair plasma state ρ_M^H . This equation shows the dark energy interacting with matter and radiation via the non-linear back-and-forth balance term $\Gamma_M(\rho_M^H - \rho_M - \rho_R)$, the massive pair plasma state ρ_M^H (2.2), and the interacting rate Γ_M (2.3), as shown in Fig. 2.

During inflation and reheating epochs, the balance term $\Gamma_M(\rho_M^H - \rho_M - \rho_R)$ is positive in Eqs. (2.5, 2.6) and (2.7). Therefore, $\dot{\rho}_\Lambda < 0$ and $\dot{\rho}_{M,R} > 0$, indicating that

dark energy converts to matter and radiation energies [47, 48]. In contrast, during standard cosmology epoch after reheating, a negative balance term for $\rho_M^H < \rho_M + \rho_R$ implies that matter and radiation convert to dark energy, resulting in $\dot{\rho}_\Lambda > 0$ [49].

In such $\tilde{\Lambda}$ CDM scenario, Eqs. (2.1-2.5) form a close set of first-order ordinary differential equations for the densities $\rho_{M,R,\Lambda}$ and Hubble function H . The solutions are completely determined, provided observations fix initial conditions and effective mass parameters. We have investigated issues such as singularity-free and large-scale anomaly, the spectral index, and tensor-to-scalar ratio relation during the inflation epoch [47]. The Universe begins ($H > \Gamma_M$) with the dark-energy $\tilde{\Lambda}$ dominated pre-inflation ($\epsilon \gtrsim 0$) and inflation ($\epsilon \approx 0.0175$), which ends ($H \approx \Gamma_M$) and transitions to the reheating. In Ref. [48], particularly Secs. 7.2-7.3, we present detailed studies of the reheating epoch where the competition between the Γ_M and Γ_M^{de} rates plays an important role. As shown in Fig. 2, the reheating starts ($\Gamma_M > H$) with the pre-reheating \mathcal{P} -episode ($\epsilon < 1$), during which dark energy rapidly converts to massive pair production and oscillation. Then, the \mathcal{M} -episode ($\epsilon \approx 3/2$) of massive pair domination occurs when $\Gamma_M > H > \Gamma_M^{\text{de}}$. This is followed by the genuine reheating \mathcal{R} -episode ($\epsilon \approx 2$) of radiation domination when $\Gamma_M^{\text{de}} > H > \Gamma_M$, during which unstable pairs decay to dark-matter particles and particles in the Standard Model for elementary particle physics. Additionally, we studied the cosmological fine-tuning and coincidence problems in the standard cosmology [49].

In this article, we investigate the dynamics and phenomena of baryogenesis and dark-matter waves based on our studies and results during the reheating epoch [48], where the plasma state mass parameter m in Eqs. (2.2) and (2.3) is specified as \hat{m} and $\hat{m} = 27.7m_{\text{pl}}$. First, we describe the particle and antiparticle density perturbation of the plasma fluid state (2.2) in the layer near the horizon, then show how the horizon crossing dynamics of these perturbation modes relate to baryogenesis, dark-matter particle-antiparticle asymmetry and dark-matter waves.

3 Particle and antiparticle density perturbations

The massive pair plasma fluid (2.2) is the “semi-classical” equilibrium state containing the same number of particles X and antiparticles \bar{X} inside the horizon, and the particle and antiparticle symmetry is preserved. However, their distributions (densities) ρ_M^\pm in spacetime are not identically in phase due to particle and antiparticle oscillations discussed in Sec. 2. Thus, the densities ρ_M^\pm and relative (contrast) density $\rho_M^+ - \rho_M^-$ do not vanish and possibly form density perturbations upon the equilibrium state (2.2) when the horizon H varies. The equilibrium state and these density perturbations have the relaxation time scale $\tau_M = \Gamma_M^{-1}$ responding to the H variation.

3.1 Equations for particle and antiparticle density perturbations

To study their relative density contrast, we separate particles from antiparticles in the massive pair plasma state (2.2), and study their density perturbations respectively and examine symmetric and asymmetric density perturbations of massive particles and antiparticles. We use the notation (+) for particles X (matter) and (−) for

antiparticles \bar{X} (antimatter). They have the same spin and mass $M \gg H$, but with opposite physical quantum numbers². They are not SM particles. However, some are unstable and decay or annihilate into SM particles and less massive dark matter particles during reheating, and stable ones remain as cold dark matter candidates.

3.1.1 Continuity and Eulerian equations

We focus on particle-antiparticle pairs' motion in the massive pair plasma layer near the horizon. Analogously to the study of cosmic perturbation, see for example [58], we separately study the linear perturbations of massive particles and antiparticles by using their continuity equation and Eulerian equations of Newtonian motion of two perfect fluids of particle (+) and antiparticle (−) densities $\rho_M^\pm(t, \mathbf{x})$, pressures $p_M^\pm(t, \mathbf{x})$ and velocities $\mathbf{v}_M^\pm(t, \mathbf{x})$ in the Robertson-Walker space-time (Freemman Universe)

$$\dot{\rho}_M^\pm + \nabla \cdot (\rho_M^\pm \mathbf{v}_M^\pm) = \Gamma_M(\rho_M^0 - \rho_M^\pm) - \Gamma_M^{\text{de}} \rho_M^\pm, \quad (3.1)$$

$$\dot{\mathbf{v}}_M^\pm + (\mathbf{v}_M^\pm \cdot \nabla) \mathbf{v}_M^\pm = -(\rho_M^\pm)^{-1} \nabla p_M^\pm - \nabla \Phi, \quad (3.2)$$

$$\nabla^2 \Phi = 4\pi G(\rho_M^+ + \rho_M^-), \quad (3.3)$$

$$\rho_M^0 = (1/2)\rho_M^H = \chi \hat{m}^2 H^2, \quad (3.4)$$

and the last line ρ_M^0 is the unperturbed mean density of equilibrium state. Note that we adopt non-relativistic equations (3.1-3.2) for the dynamics of particle and antiparticle perfect fluids since they are very massive and non-relativistic. The densities $\rho_M^\pm \sim p_M^H$ and pressures $p_M^\pm \sim p_M^H$ are components of the massive plasma fluid (2.2) with an equation of state $p_M^H = \omega_M^H \rho_M^H$ and $\omega_M^H \ll 1$. These equations are valid only inside the horizon, where the causality for these equations holds. The characteristic time scale of perturbation equations (3.1) and (3.2) relates to the relaxation time scale $\tau_M = \Gamma_M^{-1}$.

In Eq. (3.1), we use the detailed balance term $\Gamma_M(\rho_M^0 - \rho_M^\pm)$ to describe fluctuating densities ρ_M^\pm around the mean density with the time scale $\tau_M = \Gamma_M^{-1}$. The term $\Gamma_M^{\text{de}} \rho_M^\pm$ describes unstable massive pair decay of the time scale $\tau_R = (\Gamma_M^{\text{de}})^{-1}$. The arguments in the above equations are comoving coordinates (\mathbf{x}, \mathbf{k}) and the time derivative and space gradients are taken with respect to the physical coordinates $(a\mathbf{x}, \mathbf{k}/a)$, where a is the scale factor. The zeroth order solutions ρ_M^\pm to Eqs. (3.1,3.2,3.3) are the mean density ρ_M^0 of massive pair plasma, which follows the Hubble flow $\mathbf{v}_M^0 = d(a\mathbf{x})/dt = H a \mathbf{x}$, and gives the gravitational potential $\Phi^0 = (2\pi G/3)\rho_M^0 |\mathbf{x}|^2$.

The interacting rates Γ_M and Γ_M^{de} , the gravitational potential Φ and mean density $\rho_M^0 = (1/2)\rho_M^H$ are invariant under the particle and antiparticle transformation. Namely, these equations are symmetric for $\rho_M^+ \leftrightarrow \rho_M^-$. Therefore, Equations (3.1-3.4) fully respect the symmetry of particle and antiparticle. We will neglect the decay term $\Gamma_M^{\text{de}} \rho_M^\pm$ by considering $\Gamma_M \gg \Gamma_M^{\text{de}}$, namely, the massive pair plasma density variation rate is much larger than the unstable pair decay rate. The argument for neglecting Γ_M^{de} will be given later in Fig. 3 caption.

²The “ \pm ” do not indicate a positive and negative electric charge, we do not use “ \dagger ” for the sake of simplifying notations.

In the density perturbation equations (3.1-3.4), the only new term is the $\Gamma_M(\rho_M^0 - \rho_M^\pm)$, compared with corresponding canonical equations in literature. This term indicates the ρ_M^\pm fluctuations upon ρ_M^0 . These fluctuations are caused by the horizon H variation in time, and the rate Γ_M quantifies their response to the horizon H variation. One should distinguish the continuum equation (3.1) from the cosmic rate equation (2.5). The former is the equation for particle (antiparticle) density perturbations inside the massive pair plasma. The latter is the equation for the massive pair plasma density interacting with the matter and dark energy densities in the Friedman equation.

3.1.2 Contrast density perturbations

Here the usual approach of density perturbation is adopted for analysis. We consider the small perturbations around the averaged mean values ρ_M^0 and \mathbf{v}_M^0 of massive pair plasma by writing

$$\delta \mathbf{v}_M^\pm = \mathbf{v}_M^\pm - \mathbf{v}_M^0, \quad \delta \rho_M^\pm = \rho_M^\pm - \rho_M^0 \quad \text{and} \quad \delta_M^\pm = \delta \rho_M^\pm / \rho_M^0. \quad (3.5)$$

They are functions of spacetime (\mathbf{x}, t) . Up to the first order in the perturbative quantities, the mean density $\rho_M^0 = \rho_M^H/2$ is approximated as a constant in spacetime, and Equations (3.1), (3.2) and (3.3) become

$$d(\delta \rho_M^\pm)/dt + \rho_M^0 \nabla \cdot (\delta \mathbf{v}_M^\pm) + 3H \delta \rho_M^\pm = -\Gamma_M \delta \rho_M^\pm, \quad (3.6)$$

$$d(\delta \mathbf{v}_M^\pm)/dt + H \delta \mathbf{v}_M^\pm = -(\rho_M^0)^{-1} \nabla \delta p_M^\pm - \nabla \delta \Phi, \quad (3.7)$$

and the Poisson equation becomes

$$\nabla^2 \delta \Phi = 4\pi G(\delta \rho_M^+ + \delta \rho_M^-). \quad (3.8)$$

In terms of $\delta_M^\pm = \delta \rho_M^\pm / \rho_M^0$, Equation (3.6) yields

$$\nabla \cdot \delta \mathbf{v}_M^\pm = -(\dot{\delta}_M^\pm + \Gamma_M \delta_M^\pm). \quad (3.9)$$

Taking the gradient of Eq. (3.7), we arrive at

$$\ddot{\delta}_M^\pm + (\Gamma_M + 2H)\dot{\delta}_M^\pm + (2H\Gamma_M + \dot{\Gamma}_M)\delta_M^\pm = v_s^2 \nabla^2 \delta_M^\pm + 4\pi G \rho_M^0 (\delta_M^+ + \delta_M^-) \quad (3.10)$$

where the sound velocity

$$v_s = (\delta p_M^\pm / \delta \rho_M^\pm)^{1/2} \quad (3.11)$$

can be obtained from the equation of state below Eq. (2.2). Since particles and antiparticles are massive, their fluid sound velocity $v_s \ll 1$ and δ_M^\pm are non-relativistic density perturbations. Equation (3.10) represents the perturbations of particle and antiparticle densities. It reduces to the usual equation for density perturbation in the case $\Gamma_M = 0$ and $\dot{\Gamma}_M = 0$. We note that (i) particle and antiparticle contrast density perturbations are treated separately; (ii) particle and antiparticle symmetry is preserved in these second-order partial differential equations at microscopic scales in time and space inside the horizon.

3.2 Equations for symmetric and asymmetric density perturbations

To describe the perturbation of the symmetric particle-antiparticle pair density, and the perturbation of the asymmetrical particle-antiparticle density, we introduce density contrasts:

$$\Delta_M \equiv (\delta_M^+ + \delta_M^-)/2 = (\rho_M^{+-} - \rho_M^H)/\rho_M^H, \quad (3.12)$$

$$\delta_M \equiv (\delta_M^+ - \delta_M^-)/2 = (\rho_M^+ - \rho_M^-)/\rho_M^H, \quad (3.13)$$

where the sum $\rho_M^{+-} \equiv \rho_M^+ + \rho_M^-$. Henceforth, we call Δ_M the pair-density ρ_M^{+-} perturbation and δ_M the particle-antiparticle-density perturbation. The Δ_M is the density contrast between perturbed pair density ρ_M^{+-} and unperturbed mean density ρ_M^H . The δ_M is the density contrast between particles' density ρ_M^+ and antiparticles' density ρ_M^- . The former is symmetric, whereas the latter is antisymmetric under the particle and antiparticle transformation $\rho_M^+ \leftrightarrow \rho_M^-$. The perturbations Δ_M and δ_M vanish, when both ρ_M^+ and ρ_M^- approach to the mean value $\rho_M^0 = (1/2)\rho_M^H$.

The vanishing perturbation $\delta_M = 0$ indicates that particle and antiparticle distributions are identical in spacetime, e.g., they are in phase. The vanishing $\Delta_M = 0$ indicates no density perturbation of massive plasma fluid (2.2) in spacetime. Instead, the non-vanishing $\delta_M \neq 0$ means that particle and antiparticle distributions are not in phase in spacetime, implying the different spatial distributions of particles and antiparticles that change in time. The non-vanishing $\Delta_M \neq 0$ implies nontrivial density perturbation upon the equilibrium state ρ_M^H (2.2). Here, we stress that the perturbations δ_M and Δ_M are not only functions of space points inside the horizon but also functions of time connecting with the horizon H evolution.

3.2.1 Acoustic wave equations

Replacing Eqs. (3.12,3.13) in Eq. (3.10), we obtain acoustic wave equations for the asymmetric δ_M and symmetric Δ_M perturbations,

$$\ddot{\delta}_M + (\Gamma_M + 2H)\dot{\delta}_M + (2H\Gamma_M + \dot{\Gamma}_M)\delta_M = v_s^2 \nabla^2 \delta_M, \quad (3.14)$$

$$\ddot{\Delta}_M + (\Gamma_M + 2H)\dot{\Delta}_M + (2H\Gamma_M + \dot{\Gamma}_M)\Delta_M = v_s^2 \nabla^2 \Delta_M + 4\pi G \rho_M^H \Delta_M. \quad (3.15)$$

It is shown that the modes Δ_M and δ_M satisfy the same type of oscillating equation, except an additional term $4\pi G \rho_M^H \Delta_M$ in Eq. (3.15) due to massive pairs in the external gravitational potential. Equations (3.14) and (3.15) are wave ($v_s \neq 1$) equation or oscillating ($v_s = 0$) equations for non-relativistic density contrast perturbations. In the inflation epoch and the \mathcal{M} -episode of the reheating, the ϵ -rate (2.4) varies slowly in time, see Fig. 2. We will neglect $\dot{\Gamma}_M = (\chi \hat{m}/4\pi)\dot{\epsilon} \gtrsim 0$.

These second-order partial differential equations (3.14) and (3.15) are valid inside the horizon and respect the asymmetry and symmetry under particle and antiparticle transformation $\rho_M^+ \leftrightarrow \rho_M^-$. They are homogeneous and linear in perturbations δ_M and Δ_M without external source terms. Their nontrivial solutions depend only on (i) the “initial” values of (δ_M, Δ_M) and $(\dot{\delta}_M, \dot{\Delta}_M)$; (ii) the boundary values of (δ_M, Δ_M) and gradients $(\nabla \delta_M, \nabla \Delta_M)$ on the horizon surface. The former can be created (triggered)

by quantum pair oscillations shown in Fig. 1, otherwise $\delta_M(\mathbf{x}, t) \equiv 0$ and $\Delta_M(\mathbf{x}, t) \equiv 0$ identically vanish in spacetime.

We define the Fourier transformation from $f_M(\mathbf{x}, t) = \Delta_M(\mathbf{x}, t), \delta_M(\mathbf{x}, t)$ to \mathbf{k} modes $f_M^{\mathbf{k}}(t) = \Delta_M^{\mathbf{k}}(t), \delta_M^{\mathbf{k}}(t)$,

$$f_M(\mathbf{x}, t) = \frac{1}{V^{1/2}} \sum_{\mathbf{k}} f_M^{\mathbf{k}}(t) e^{i\mathbf{k}\mathbf{x}}, \quad (3.16)$$

$$f_M^{\mathbf{k}}(t) = \frac{1}{V^{1/2}} \int d^3x f_M(\mathbf{x}, t) e^{-i\mathbf{k}\mathbf{x}}, \quad (3.17)$$

where $V = (4\pi/3)H^{-3}$ is the physical Hubble volume. The corresponding wave-propagating equations for \mathbf{k} -modes' $\delta_M^{\mathbf{k}}$ and $\Delta_M^{\mathbf{k}}$ are approximately given by,

$$\ddot{\delta}_M^{\mathbf{k}} + (\Gamma_M + 2H)\dot{\delta}_M^{\mathbf{k}} + 2H\Gamma_M\delta_M^{\mathbf{k}} + (v_s^2|\mathbf{k}|^2/a^2)\delta_M^{\mathbf{k}} = 0 \quad (3.18)$$

$$\ddot{\Delta}_M^{\mathbf{k}} + (\Gamma_M + 2H)\dot{\Delta}_M^{\mathbf{k}} + 2H\Gamma_M\Delta_M^{\mathbf{k}} + (v_s^2|\mathbf{k}|^2/a^2)\Delta_M^{\mathbf{k}} = 4\pi G\rho_M^H\Delta_M^{\mathbf{k}}. \quad (3.19)$$

These are semi-classical equations governing the oscillating modes $\delta_M^{\mathbf{k}}$ and $\Delta_M^{\mathbf{k}}$ of effective frequencies

$$\omega_\delta^2(\mathbf{k}) = 2H\Gamma_M + (v_s^2|\mathbf{k}|^2/a^2) \quad (3.20)$$

$$\omega_\Delta^2(\mathbf{k}) = 2H\Gamma_M + (v_s^2|\mathbf{k}|^2/a^2) - 4\pi G\rho_M^H. \quad (3.21)$$

The Γ_M -term contributes to the friction coefficient $(\Gamma_M + 2H)$ in oscillation equations and “quasi mass” term $(2H\Gamma_M)^{1/2}$ in the oscillation frequency $\omega_{\delta,\Delta}^2(\mathbf{k})$. The fast oscillating perturbation modes $\delta(\mathbf{k})$ and $\Delta(\mathbf{k})$ have a small time scale $\omega_{\delta,\Delta}^{-1}(\mathbf{k}) \leq (2H\Gamma_M)^{-1/2}$. Here, we consider an adiabatic approximation of $H\Gamma_M$ being almost constant on such a small time scale. The reason is that H and Γ_M are slowly time-varying functions governed by the Freedman equation (2.1) and cosmic rate equations (2.5, 2.6) in macroscopic time scales τ_H and τ_M , see the reheating \mathcal{M} -episode in Fig. 2.

The term $4\pi G\rho_M^H$ in Eqs. (3.19, 3.21) could lead to the Jeans instability, due to the gravitational attraction of massive pair plasma, possibly giving a nontrivial solution Δ_M . Observe that in Eq. (3.21) $4\pi G\rho_M^H = 8\pi\chi(\hat{m}/M_{\text{pl}})^2H^2$ is much smaller than $2H\Gamma_M + (v_s^2|\mathbf{k}|^2/a^2)$ even for the case $|\mathbf{k}| = 0$ and $\hat{m} \gg H$ ($v_s^2 \ll 1$) in the inflation and reheating epochs, as well as standard cosmology. Therefore the negative term $4\pi G\rho_M^H$ can be neglected and $\omega_\Delta^2(\mathbf{k}) > 0$, implying the Jeans instability should not occur in these epochs.

3.2.2 Lowest-lying mode oscillating equations

We will discuss the solutions to Eqs. (3.18-3.21) for the density perturbations in the inflation epoch and three episodes \mathcal{P} , \mathcal{M} and \mathcal{R} of the reheating epoch, see Fig. 2. We first focus on the lowest-lying oscillation modes by neglecting the pressure term $v_s^2\nabla^2$ or $(v_s^2|\mathbf{k}|^2/a^2)$ terms for wave propagation, since massive pairs' plasma fluid (2.2) is non-relativistic and their sound velocity is small $v_s^2 \ll 1$. Equations (3.18-3.21) become oscillating equations,

$$\ddot{\delta}_M^0 + (\Gamma_M + 2H)\dot{\delta}_M^0 + 2H\Gamma_M\delta_M^0 = 0, \quad (3.22)$$

$$\ddot{\Delta}_M^0 + (\Gamma_M + 2H)\dot{\Delta}_M^0 + 2H\Gamma_M\Delta_M^0 = 0, \quad (3.23)$$

where the lowest lying oscillation modes $\delta_M^0 \equiv \delta_M^{\mathbf{k}=0}$ and $\Delta_M^0 \equiv \Delta_M^{\mathbf{k}=0}$ with the frequencies $\omega_\delta \equiv \omega_\delta(|\mathbf{k}|=0)$ and $\omega_\Delta \equiv \omega_\Delta(|\mathbf{k}|=0)$,

$$\omega_\delta^2 = \omega_\Delta^2 = 2H\Gamma_M. \quad (3.24)$$

We call the lowest-lying modes as “zero modes” Δ_M^0 and δ_M^0 of pair-density and particle-antiparticle-density oscillations. In this semi-classical approximation, these zero modes’ frequency (3.24) weakly depend on the time t in the period of slowly time-varying H and Γ_M .

We note that Eqs. (3.22) and (3.23) have the same structure, and they are no longer oscillating equations when $\Gamma_M = 0$, namely, microscopic pair oscillations decouple from the macroscopic horizon evolution. In this case, the solutions damp in time, $\Delta_M^0 \rightarrow 0$ and $\delta_M^0 \rightarrow 0$. Namely, $\rho_M^+, \rho_M^- \rightarrow \rho_M^0$ and $\rho_M^{+-} \rightarrow \rho_M^H$, see Eqs. (3.12) and (3.13), density perturbations do not occur. As will be seen, $\Gamma_M \neq 0$ is crucial for discussing density perturbation dynamics in this article.

To end this section, we would like to mention that the oscillations δ_M^0 are the spatial fluctuations in the number of particles or antiparticles (compositions) per comoving volume, and the oscillations Δ_M^0 are the spatial fluctuations in the number of pairs per comoving volume.

3.2.3 Particle-antiparticle asymmetry due to modes’ horizon crossing

Before analyzing acoustic wave equations (3.14) and (3.15) in the coordinate space \mathbf{x} or their counterparts (3.18) and (3.19) in the momentum space \mathbf{k} , we discuss in general the possible situations for nontrivial particle-antiparticle asymmetric solutions inside the horizon due to modes’ horizon crossing.

The local and instantaneous perturbations of relative density $\delta_M(\mathbf{x}, t) \neq 0$ produced by quantum pair oscillations (Fig. 1) is necessary but not sufficient for creating particle and antiparticle asymmetry, namely net particle numbers observed inside the horizon. We need to examine the total net particle numbers $\int_V d^3x \rho_M^H \delta_M = \hat{m}(N^+ - N^-) \equiv D_{+-}$, where N^\pm are the total numbers of particles and antiparticles inside the horizon. Integrating Eq. (3.14) overall the horizon volume V , we obtain inside the horizon,

$$\begin{aligned} \ddot{D}_{+-} + (\Gamma_M + 2H)\dot{D}_{+-} + (2H\Gamma_M + \dot{\Gamma}_M)D_{+-} \\ = v_s^2 \int_V d^3x \nabla^2(\delta_M \rho_M^H) = v_s^2 \int_{\partial V} d\mathbf{S} \cdot \nabla(\delta_M \rho_M^H), \end{aligned} \quad (3.25)$$

where the right-handed side for $\nabla(\delta_M \rho_M^H)|_{\partial V} \neq 0$ and $\delta_M|_{\partial V} \neq 0$ represents the difference of particles and antiparticles crossing in or out the horizon surface ∂V of the horizon volume V .

In our framework, there is no any nontrivial “initial” values $\dot{D}_{+-}^0 \neq 0$ and $D_{+-}^0 \neq 0$ caused by the external sources of particle and antiparticle asymmetric interactions and processes because of no explicit or spontaneous breaking of particle and antiparticle symmetry in microscopic interactions. However, there are the local relative (contrast)

densities $\delta_M^{\mathbf{k}} \neq 0$, which are caused by quantum pair oscillations (Fig. 1) of particle and antiparticle production, kinetic motion and annihilation inside the horizon.

Thus, in this framework “initial” values $\dot{D}_{+-}^0 = 0$ and $D_{+-}^0 = 0$ of particles and antiparticles vanish inside the horizon, but their local relative contrast perturbations $\delta_M(\mathbf{x}, t) \neq 0$ are nontrivial in spacetime. We discuss the possibilities of nontrivial asymmetric solution $\dot{D}_{+-}(t) \neq 0$ and $D_{+-}(t) \neq 0$ appearing inside the horizon as the horizon H evolves in time:

- (a) the trivial boundary values $\nabla(\delta_M \rho_M^H)|_{\partial V} = 0$ and $\delta_M|_{\partial V} = 0$, representing there is no particle-antiparticle horizon crossing. It means in momentum mode space (3.18), all $\delta_M^{\mathbf{k}}$ modes’ wavelength $\omega_\delta^{-1}(\mathbf{k})$ (3.20) are smaller than the horizon size H^{-1} , i.e., $\omega_\delta(\mathbf{k}) > H$. All modes $\delta_M^{\mathbf{k}}$ are inside the horizon. As a result of linear and homogeneous Eq. (3.25), $\dot{D}_{+-}(t) = 0$ and $D_{+-}(t) = 0$, no particle-antiparticle asymmetry occurs inside the horizon of the volume V , which contains all particles and antiparticles $N^+ \equiv N^-$.
- (b) the nontrivial boundary values $\nabla(\delta_M \rho_M^H)|_{\partial V} \neq 0$ and $\delta_M|_{\partial V} \neq 0$, representing the particle-antiparticle horizon crossing. It means in momentum mode space (3.18) some $\delta_M^{\mathbf{k}}$ modes’ wavelength $\omega_\delta^{-1}(\mathbf{k})$ (3.20) exceeds the horizon size H^{-1} , i.e., $\omega_\delta(\mathbf{k}) < H$, thus they cross outside the horizon. Nontrivial boundary conditions or non-vanishing right-handed side of Eq. (3.25) implies that $\dot{D}_{+-}(t) \neq 0$ and $D_{+-}(t) \neq 0$ and particle-antiparticle asymmetry can possibly occur inside the horizon. However, the total number of particles inside and outside the horizon conserves,

$$\int_V d^3x \rho_M^H \delta_M + \int_{V_{\text{out}}} d^3x \rho_M^H \delta_M \equiv 0, \quad (3.26)$$

where the second term $\int_{V_{\text{out}}} d^3x \rho_M^H \delta_M = D_{+-}^{\text{out}} = \hat{m}(N_{\text{out}}^+ - N_{\text{out}}^-)$ represents the difference between particles and antiparticles outside the horizon V_{out} . The sub-horizon observers see the particle-antiparticle asymmetry $D_{+-} = -D_{+-}^{\text{out}} \neq 0$, whose value relates to crossing-mode $\delta_M|_{\omega_\delta(\mathbf{k})=H}$ amplitudes on the horizon surface ∂V at the horizon-crossing moment. The horizon boundary term on the right-handed side of Eq. (3.25) is proportional to

$$4\pi H^{-2} \rho_M^H H \delta_M|_{\partial V} = 8\pi \chi \hat{m}^2 H \delta_M|_{\partial V}, \quad (3.27)$$

which is nontrivial as long as $\delta_M|_{\partial V} \neq 0$.

Similar discussions also apply to Eq. (3.15) for the density perturbation Δ_M , which we omit here to simplify the text. The above discussions are essentially same as those, see below Eqs. (3.14) and (3.15) on initial and boundary conditions necessary for nontrivial solutions to second-order partial differential equations. We thus turn to the discussions of the horizon-crossing possibility (b) of the difference between particle and antiparticle modes crossing the horizon surface in the following two distinct cases.

First, in the case of horizon $H = \text{const}$ and volume V fixed in time and $\Gamma_M = 0$, Eqs. (3.14) and (3.18) become usual equations for perturbations

$$\ddot{\delta}_M + 2H\dot{\delta}_M - v_s^2 \nabla^2 \delta_M = 0. \quad (3.28)$$

The particle and antiparticle symmetry $D_{+-} = 0$ holds inside the horizon, assuming particle-antiparticle oscillations δ_M are confined inside the horizon $\delta_M|_{\partial V} = 0$ and $\nabla(\delta_M \rho_M^H)|_{\partial V} = 0$. All sub-horizon modes $\delta_M^{\mathbf{k}}$ obey the wave-mode equation

$$\ddot{\delta}_M^{\mathbf{k}} + 2H\dot{\delta}_M^{\mathbf{k}} + (v_s^2 |\mathbf{k}|^2 / a^2) \delta_M^{\mathbf{k}} = 0, \quad (3.29)$$

with physical wavelength $\omega_{\delta, \Delta}^{-1}(\mathbf{k}) = (v_s |\mathbf{k}| / a)^{-1} < H^{-1}$. This sub-horizon condition does not change in time, which is the crucial point. Therefore, the particle and antiparticle symmetry $D_{+-}(t) = 0$ preserves in time. Moreover, the relative density perturbations δ_M or modes $\delta_M^{\mathbf{k}}$ inside the horizon $\delta_M, \delta_M^{\mathbf{k}} \propto e^{-Ht}$ dampen down in time. The similar discussion applies to Eq. (3.23) for the density perturbations $\Delta_M^{\mathbf{k}}$, if we neglect the small gravitational attraction term $4\pi G \rho_M^H \Delta_M^{\mathbf{k}}$.

Second, we come to the case that slowly time-varying H and $\Gamma_M \neq 0$ are present in adiabatically approximated wave-mode equations (3.18) and (3.19). The effective frequencies (3.20) and (3.21) are time dependent via the quasi mass term $2H\Gamma_M$. Therefore, the sub-horizon condition $\omega_{\delta}^{-1}(\mathbf{k}) < H^{-1}$ can change to the super-horizon condition $\omega_{\delta}^{-1}(\mathbf{k}) > H^{-1}$ in time, *vice versa*. Thus there is a possibility in time evolution that the symmetric $D_{+-} = 0$ case of *all* particle and antiparticle oscillating modes inside the horizon (sub-horizon) can change to the asymmetric $D_{+-} \neq 0$ case of some modes outside the horizon (super-horizon) at the horizon crossing $\omega_{\delta}^{-1}(\mathbf{k}) = H^{-1}$, *vice versa*. Namely, as the horizon H and rate Γ_M evolve in time, the aforementioned sub-horizon case (a) and the super-horizon case (b) exchange. As a consequence, some particles or antiparticles cross in or out the horizon surface ∂V and $\nabla(\delta_M \rho_M^H)|_{\partial V} \neq 0$ in Eq. (3.25).

In other words, due to the horizon-expanding and spacetime strengthening, particles and antiparticles decouple from oscillating each other, causing the possibility that particles remain inside the horizon and antiparticles go outside the horizon. Particles or antiparticles that cross outside the horizon are out of causality, and their oscillating amplitudes $\delta_M^{\mathbf{k}}$ are frozen, and the values depend on when the horizon-crossing occurs. On the contrary, in time evolution, there is also the possibility that antiparticle (particle) super-horizon modes return to the horizon and couple to particle (antiparticle) modes, undergoing sub-horizon pair oscillation modes.

Moreover, the massive pair plasma fluid (2.2) is an holographic layer near the horizon H , which evolves on the time scale $\tau_H = H^{-1} \gg \tau_M$. During the horizon evolution, the particle and antiparticle relative density perturbation modes can cross the horizon, depending on their wavelength compared with the horizon size. It is a dynamic of competition between the horizon-expanding rate H and the particle-antiparticle oscillation rate $\omega_{\delta, \Delta}(\mathbf{k})$. In a semi-classical picture, this dynamical phenomenon illustrates when spacetime expands so fast that particle and antiparticle pairs do not have enough time to proceed with their back-and-forth oscillations, thus decoupling from each other. Therefore, particles (or antiparticles) go out of the horizon, and their partners remain

inside the horizon. Similar dynamics are studied in the neutrinos decoupling [59] in the early Universe and electrons and positrons decoupling in their pair plasma undergoing an ultra-relativistic hydrodynamical expansion [60–62].

In the next sections, we attempt to study such horizon-crossing dynamics of massive pair plasma oscillations, i.e., the sub-horizon case (a) and super-horizon case (b), in the reheating epoch to see possible physical consequences.

4 Particle-antiparticle oscillation and horizon crossing

To study how horizon-crossing modes produce particle-antiparticle asymmetry, we first recall the usual approach to study the curvature (metric) perturbations $\delta\phi$ and their horizon crossings, which cause density perturbations for large-scale structure and galaxy formation, for example, [58]. Microscopic physics causally operates only on distance scales less than the Hubble radius, as the Hubble radius represents the distance a light signal can travel in an expansion time $\tau_H = H^{-1}$. As a microscopic mode $\delta\phi_k$ of physical wavelength $(k/a)^{-1} > H^{-1}$, it crosses outside the horizon, decouples from microphysics and freezes in as a classical field $\delta\phi_k \approx \text{constant}$. It is the phenomenon of microscopic mode $\delta\phi_k$ super-horizon crossing. When its physical wavelength $(k/a)^{-1} < H^{-1}$, the frozen mode reenters the horizon and returns to the fluctuating field coupling to microphysics. Such sub-horizon crossing phenomenon causes density perturbations for large-scale structure and galaxy formation. The perturbation mode super- or sub-horizon crossing is a dynamical process competition between the microscopic physics scale and the macroscopic horizon H scale varying in time.

Instead of the curvature perturbation modes $\delta\phi_k$, we study the similar dynamics and phenomenon for the density contrast perturbation modes $\delta_M^{\mathbf{k}}$ (3.18) and $\Delta_M^{\mathbf{k}}$ (3.19) whose microscopic physics scales are frequencies (3.20, 3.21). The $\delta_M^0 \neq 0$ ($\delta_M^0 = 0$) inside the horizon implies massive particle X and antiparticle \bar{X} asymmetry (symmetry). We will show their super- and sub-horizon crossings phenomena possibly accounting for dark-matter particle and antiparticle asymmetry and baryogenesis.

4.1 Under- and over-damped oscillating modes

We start with the analysis for the lowest-lying modes δ_M^0 and Δ_M^0 of Eqs. (3.22–3.24). In general, we expect that for large frequencies $\omega_{\delta,\Delta} \gg (\Gamma_M + 2H)$, the modes δ_M^0 and Δ_M^0 are underdamped oscillating inside the horizon. While small frequencies $\omega_{\delta,\Delta} \ll (\Gamma_M + 2H)$, the friction term $(\Gamma_M + 2H)\dot{\delta}_M^0$ dominates, the amplitudes of the modes δ_M^0 and Δ_M^0 are overdamped and frozen to be constants outside the horizon $\delta_M^0 \rightarrow \text{const}$ and $\Delta_M^0 \rightarrow \text{const}$, decoupling from microscopic physics. Horizon crossing occurs at $\omega_{\delta,\Delta} \approx (\Gamma_M + 2H)$. Following the usual approach for curvature perturbations, we present a quantitative analysis to show the horizon-crossing phenomenon by using the simplified Eqs. (3.22, 3.23) and (3.24) in one dimension and assuming isotropic three-dimension oscillations.

In terms of dimensionless variables $t \rightarrow \hat{m}t$, $\Gamma_M \rightarrow \Gamma_M/\hat{m}$ and $H \rightarrow H/\hat{m}$, we rewrite Eq. (3.22) in the form of the usual equation for a dampened harmonic oscillator,

$$\ddot{\delta}_M^0 + 2\zeta\omega_\delta\dot{\delta}_M^0 + \omega_\delta^2\delta_M^0 = 0, \quad (4.1)$$

and the same for the mode Δ_M^0 . The underdamped frequency ω_δ and the damping ratio ζ are,

$$\omega_\delta^2 \equiv 2\Gamma_M H, \quad \zeta \equiv (\Gamma_M + 2H)/(2\omega_\delta), \quad (4.2)$$

where $\Gamma_M = \chi \hat{m} \epsilon / (4\pi)$ (2.3) is almost a constant in time, see Fig. 2 for the \mathcal{M} -episode of the reheating epoch, and H -variation has the time scale $\tau_M = H^{-1}$ from the Friedman equations (2.1) in the reheating epoch. Thus, in the oscillating equation (4.2), ω_δ^2 and $2\zeta\omega_\delta$ are slowly time-varying functions in the period of the time-oscillating modes Δ_M^0 and δ_M^0 , the same discussions apply to high-energy modes $|\mathbf{k}|$.

When $\Gamma_M = 0$ and $\omega_\delta = 0$, Eq. (4.1) yields a damping solution $\delta_M^0 \propto e^{-Ht} \rightarrow 0$ in time, and same discussions for Δ_M^0 . There are no dynamics of δ_M^0 and Δ_M^0 modes' oscillating and horizon crossing. The new term $\Gamma_M \neq 0$ determines modes' frequency and damping (4.2) in comparison with the Hubble rate H of horizon expansion. Thus, it plays a crucial role in the following discussions and results of producing particle and antiparticle asymmetry.

We further approximately treat the slowly time-varying ω_δ^2 and $2\omega_\delta\zeta$ as constants in time. In this circumstance, the approximate solution to Eq. (4.1) reads

$$\delta_M^0 \propto e^{-\omega_\delta\zeta t} e^{-i\omega_\delta(1-\zeta^2)^{1/2}t}. \quad (4.3)$$

We have the following physical situations:

- (i) in the underdamped case ($\zeta < 1$), i.e., $2\omega_\delta > \Gamma_M + 2H$, the modes δ_M^0 and Δ_M^0 oscillate with smaller frequencies than ω_δ , their wavelengths are smaller than the horizon size, and amplitudes damped to zero inside the horizon. This underdamped case corresponds to the non-horizon-crossing case, i.e., the sub-horizon case (a) below Eq. (3.25). No particle-antiparticle asymmetry is produced inside the horizon. The damping time scale $(\omega_\delta\zeta)^{-1} = (\Gamma_M + H)^{-1} \approx \Gamma_M^{-1}$.
- (ii) in the overdamped case ($\zeta > 1$), i.e., $2\omega_\delta < \Gamma_M + 2H$, the δ_M^0 and Δ_M^0 modes' wavelengths are larger than the horizon size, and their amplitudes exponentially decay and return to steady states without oscillating. This overdamped case corresponds to the horizon-crossing case, i.e., the super-horizon case (b) below Eq. (3.25). In the case ($\zeta \gg 1$), the solution (4.3) yields $\delta_M^0, \Delta_M^0 \propto \text{const.}$, indicating the amplitudes of modes δ_M^0 and Δ_M^0 are "frozen" to constants outside the horizon. It implies that the particle-antiparticle asymmetry could be produced inside the Horizon, as discussed below.

4.2 Lowest-lying oscillation mode crossing horizon

The separatrix between two situations (i) and (ii) is defined at $\zeta = 1$. At this separatrix, the frequency ω_δ and damping ratio ζ (4.2) lead to

$$\Gamma_M = 2H, \quad (4.4)$$

and the critical ratio of horizon radius and pair oscillating length

$$\frac{H^{-1}}{\omega_{\delta}^{-1}} = \left(\frac{2\Gamma_M}{H} \right)^{1/2} = 2. \quad (4.5)$$

Such a critical ratio represents the horizon crossing of the zero modes δ_M^0 and Δ_M^0 :

- (a) subhorizon δ_M^0 and Δ_M^0 modes are *inside* the horizon for $(H^{-1}/\omega_{\delta}^{-1}) > 2$;
- (b) superhorizon δ_M^0 and Δ_M^0 modes are *outside* the horizon for $(H^{-1}/\omega_{\delta}^{-1}) < 2$.

These results have clear physical meanings. Whether the oscillating modes are the subhorizon size or superhorizon size crucially depends on the “time-competition” (4.4) between the density perturbations ($\rho_M^{\pm} \Leftrightarrow \rho_M^0$) rate Γ_M and the Hubble rate H of spacetime expansion: $\Gamma_M > H$ the modes stay inside the horizon; $\Gamma_M < H$ the modes stay outside the horizon. In other words, the modes stay inside (outside) the horizon, if they oscillate faster (slower) than the spacetime expanding rate, since they have (no) enough time to keep themselves inside the horizon. Consistently, the “space-competition” ratio (4.5) of horizon size and mode wavelength shows (a) subhorizon-sized modes and (b) superhorizon-sized modes.

The horizon crossing condition (4.5) clearly depends on the functions $H(t)$ and $\Gamma_M(t)$ in different epochs of the Universe evolution. At the horizon crossing (4.5), the rate (2.3) is $\Gamma_M^{\text{cr}} = \chi \hat{m} \epsilon_{\text{cr}} / (4\pi)$, we find the horizon crossing condition $H_{\text{cr}} = \Gamma_M^{\text{cr}} / 2$ (4.4) for the zero mode

$$(H_{\text{cr}} / \chi \hat{m}) = (1/8\pi) \epsilon_{\text{cr}}, \quad (4.6)$$

where H_{cr} and ϵ_{cr} stand for the Hubble rate and ϵ -rate at the horizon crossing. The LHS of Eq. (4.6) is the ratio of massive pair plasma layer width and horizon radius, e.g., $(\lambda_m / H_{\text{cr}}^{-1})$. While the RHS of Eq. (4.6) is the ϵ -rate (2.4) depending on the horizon evolution. They are equal when the horizon crossing occurs.

5 Oscillating amplitudes at horizon crossing

To quantify symmetric and asymmetric oscillating amplitudes at horizon crossing, we define the root-mean-square (*rms*) density fluctuations by

$$\bar{\delta}_M \equiv \langle \delta_M(\mathbf{x}) \delta_M^{\dagger}(\mathbf{x}) \rangle^{1/2}, \quad \bar{\Delta}_M \equiv \langle \Delta_M(\mathbf{x}) \Delta_M^{\dagger}(\mathbf{x}) \rangle^{1/2} \quad (5.1)$$

where $\langle \dots \rangle = V^{-1} \int d^3x (\dots)$ indicates the average all states over the space. The use of Fourier transformations (3.16) and (3.17) yields

$$\bar{\delta}_M^2 = \frac{1}{V} \sum_{\mathbf{k}, \mathbf{k}'} \delta_M^{\mathbf{k}} \delta_M^{\mathbf{k}'\dagger} \delta_{\mathbf{k}, \mathbf{k}'} = \frac{1}{V} \sum_{\mathbf{k}} |\delta_M^{\mathbf{k}}|^2 \quad (5.2)$$

and the same for $\bar{\Delta}_M^2$, where the dimensionless $\delta_{\mathbf{k}, \mathbf{k}'} = V^{-1} \int d^3x e^{i\mathbf{x}(\mathbf{k}-\mathbf{k}')} \delta_{\mathbf{k}, \mathbf{k}'}$ is the Kronecker delta function of discrete variables \mathbf{k} and \mathbf{k}' .

5.1 Lowest-lying mode amplitudes at horizon crossing

Considering contribution only from the lowest-lying modes (ground state) of underdamped oscillating δ_M^0 and Δ_M^0 , we approximately obtain from Eq. (5.2)

$$\bar{\delta}_M^2 \approx V^{-1} |\delta_M^0|^2, \quad \bar{\Delta}_M^2 \approx V^{-1} |\Delta_M^0|^2. \quad (5.3)$$

At a fixed time t , the amplitudes $|\delta_M^0|^2$ and $|\Delta_M^0|^2$ of the lowest-lying modes of the underdamped harmonic oscillator (4.1) can be expressed by the oscillation characteristic length scale $1/(2\hat{m}\omega_{\delta,\Delta})^{1/2}$,

$$|\delta_M^0|^2 \approx 1/(2\hat{m}\omega_\delta)^{3/2}, \quad |\Delta_M^0|^2 \approx 1/(2\hat{m}\omega_\Delta)^{3/2}, \quad (5.4)$$

see, e.g., Refs. [63], [64] and [65]. If the wavelength of the lowest-lying mode is much smaller than the horizon radius, the mode will evolve adiabatically, and Eq. (5.4) will continue to hold at later times. From Eq. (5.3), we obtain the root-mean-square of density fluctuations

$$\bar{\delta}_M^2 = \bar{\Delta}_M^2 \approx \frac{1}{4\pi(2\hat{m})^{3/2}} \frac{3H^3}{(2H\Gamma_M)^{3/4}}. \quad (5.5)$$

At the other extreme, if the wavelength of the lowest-lying mode is much larger than the horizon radius, the oscillator will overdamp, and the oscillating amplitudes $\bar{\delta}_M$ and $\bar{\Delta}_M$ will remain constants in time. These constants at the horizon crossing $H_{\text{cr}} = \Gamma_M^{\text{cr}}/2$ (4.6) are

$$\bar{\delta}_M = \bar{\Delta}_M \approx \left(\frac{3}{32\pi}\right)^{1/2} \left(\frac{H_{\text{cr}}}{\hat{m}}\right)^{3/4} = \left(\frac{3}{32\pi}\right)^{1/2} \left(\frac{\chi\epsilon_{\text{cr}}}{8\pi}\right)^{3/4}, \quad (5.6)$$

whose values depend on the Hubble rate H or the ϵ -rate values at the horizon crossing.

5.2 Particle-antiparticle asymmetry due to horizon crossing

As a result, using Eqs. (3.12,3.13), we explicitly write the result (5.6) as,

$$\rho_M^+ - \rho_M^- = \bar{\delta}_M \rho_M^H, \quad (5.7)$$

$$\rho_M - \rho_M^H = \bar{\Delta}_M \rho_M^H, \quad (5.8)$$

where the right-handed sides are in the sense of *rms*. In other words, $\bar{\delta}_M \rho_M^H$ represents the spatial fluctuations in the number of particles or antiparticles (compositions) per comoving volume, and $\bar{\Delta}_M \rho_M^H$ represents the spatial fluctuations in the number of pairs per comoving volume. This result physically implies the following two consequences due to the particle-antiparticle oscillations at the horizon crossing:

- (i) In the case that the δ_M^0 is an underdamped oscillating mode inside the horizon, its root-mean-squared (*rms*) value $\bar{\delta}_M$ vanishes, indicating all particles and antiparticles are inside the horizon, no net particle number appears with respect to a subhorizon observer, i.e., an observer inside the horizon. This underdamped case corresponds to the non-horizon-crossing case (i) below Eq. (4.3) and the subhorizon case (a) below Eq. (3.25). There is no particle-antiparticle asymmetry inside the horizon.

- (ii) In the case that the δ_M^0 is an overdamped oscillating mode frozen outside the horizon, its root-mean-squared (*rms*) value $\bar{\delta}_M$ does not vanish. It indicates that some particles (or antiparticles) are outside the horizon. Thus net particle number appears with respect to the subhorizon observer. This overdamped case corresponds to the horizon-crossing case (ii) below Eq. (4.3) and the super-horizon case (b) below Eq. (3.25). There is a particle-antiparticle asymmetry inside the horizon. Note that the “frozen” amplitudes of $\bar{\delta}_M$ and $\bar{\Delta}_M$ (5.6) are very small for $\hat{m} \gg H_{\text{cr}}$.

It is important to note that the summed number of particles and antiparticles inside and outside the horizon is zero in both cases, as required by total particle number conservation. In the second case (ii), the positive (negative) net number of particles and antiparticles viewed by the subhorizon observer is equal to the negative (positive) net number of particles and antiparticles outside the horizon. The asymmetric perturbation $\bar{\delta}_M$ occurring at the horizon crossing describes particle and antiparticle number asymmetry inside the horizon.

The lowest-lying mode δ_M^0 inside the horizon represents an under-damping oscillation between particles and antiparticles and its dampened amplitude vanishes within the horizon. As a result, the averaged net number of particles is zero at the time period $t \sim H^{-1}$, and particle and antiparticle symmetry is preserved. Instead, the lowest-lying mode δ_M outside the horizon means that its amplitude is frozen to a constant $\delta_M^0 = \text{const.} \neq 0$. This implies that the subhorizon observer should observe a non-vanishing net particle number associating the horizon surface, representing the modes of constant amplitude outside the horizon. Such mode horizon crossing indicates the occurrence of particle and antiparticle asymmetry. The same discussions apply to the pair-density perturbation mode Δ_M^0 (3.12), which however does not violate the symmetry of particle and antiparticle. In the next section, we must examine when such mode horizon crossing occurs in the reheating epoch.

6 Subhorizon crossing in pre-reheating

To identify the subhorizon crossing at preheating \mathcal{P} -episode, when the reheating starts, we examine that (i) the modes δ_M^0 and Δ_M^0 are superhorizon size in the pre-inflation and inflation epochs before the \mathcal{P} -episode; (ii) they become subhorizon size in the massive pair oscillating \mathcal{M} -episode, after the \mathcal{P} -episode, see Fig. 2.

6.1 Particle-antiparticle asymmetry in pre-inflation and inflation

In the pre-inflation and inflation epoch $H > \Gamma_M$ and $\epsilon \ll 1$, when $x = \ln(a/a_{\text{end}}) \leq 10^{-3}$ in Fig. 2, the modes δ_M^0 and Δ_M^0 are outside the horizon, corresponding to the overdamped case ($\zeta > 1$). This can also be seen by the ratio of horizon radius H^{-1} and pair oscillating length ω_δ^{-1} (3.24),

$$\frac{H^{-1}}{\omega_\delta^{-1}} = \left(\frac{H^{-2}}{2^{-1}\Gamma_M^{-1}H^{-1}} \right)^{1/2} < \left(\frac{\Gamma_M^{-1}}{2^{-1}\Gamma_M^{-1}} \right)^{1/2} = 2^{1/2}, \quad (6.1)$$

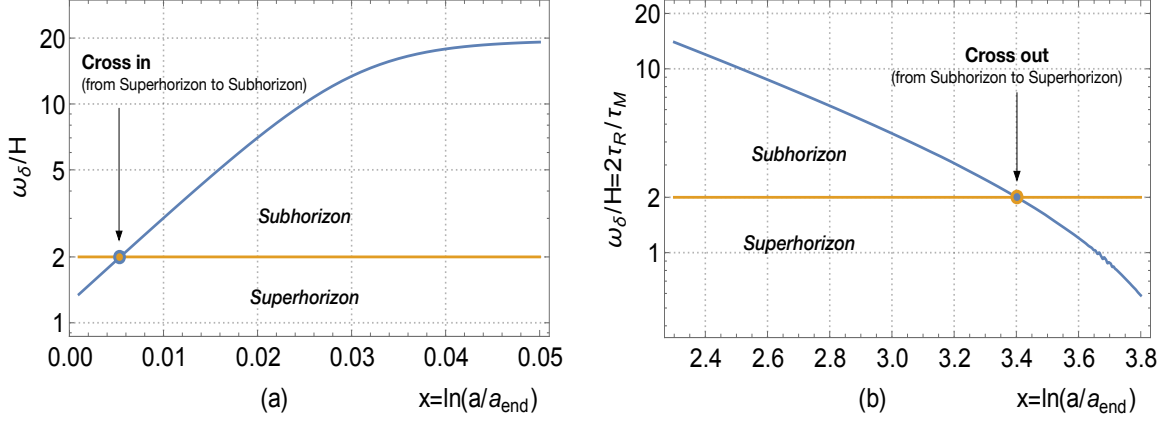


Figure 3. (Color Online). In these two figures (a) and (b), we use the previous numerical results H and Γ_M obtained by solving Eqs. (6.6-6.11) with the parameters $\hat{m}/m_{\text{pl}} = 27.7$ and $g_Y^2 = 10^{-9}$ in Ref. [48]. In terms of the e -folding number $x = \ln(a/a_{\text{end}})$, the ratio ω_δ/H (6.2) of the horizon size H^{-1} and the oscillating length ω_δ^{-1} is plotted (blue), compared with the horizon crossing $\omega_\delta/H = 2$ (orange). The superhorizon (subhorizon) is below (above) the orange horizontal line. Left (a): The ratio $\omega_\delta/H = (2\Gamma_M/H)^{1/2}$ (4.5) (blue) in the preheating \mathcal{P} -episode. The modes (blue line) evolve from superhorizon to subhorizon and cross at $\ln(a_{\text{crin}}/a_{\text{end}}) \approx 0.005$ and $a_{\text{crin}} \approx 1.01 a_{\text{end}}$. Right (b): The ratio $\omega_\delta/H \approx (2\tau_R/\tau_M)$ (7.2) (blue) in the genuine reheating \mathcal{R} -episode. The modes (blue line) evolve from subhorizon to superhorizon and cross at $\ln(a_{\text{crou}}/a_{\text{end}}) \approx 3.4$ and $a_{\text{crou}} \approx 30a_{\text{end}}$. Whereas, the reheating occurs at $\ln(a_R/a_{\text{end}}) \approx 3.8$ and $a_R \approx 45 a_{\text{end}}$ from Fig. 7 (a) of Ref. [48]. Thus, $a_{\text{crou}} \lesssim a_R$. It shows the crossing occurs before the massive pair domination (\mathcal{M} -episode) ends. This is the reason that we neglect the decay rate $\dot{\Gamma}^{\text{de}} \ll \Gamma_M$ in analyzing Eq. (3.1). Also we neglect the term $\dot{\Gamma}_M \propto \epsilon \approx 0$ in acoustic equations (3.14,3.15), since the subhorizon crossing is near inflation end and the superhorizon crossing is near \mathcal{M} -episode end where $\epsilon \approx 0$.

indicating $H^{-1}/\omega_\delta^{-1} < 2$. We use the numerical results in Ref. [48] to show the ratio (6.1) in Fig. 3 (a), where the blue line $H^{-1}/\omega_\delta^{-1}$ is below the orange line 2. This implies that in the pre-inflation and inflation, the modes δ_M^0 and Δ_M^0 wavelengths are larger than the horizon size, their amplitudes exponentially decay and return to steady states without oscillating. It means that the modes δ_M^0 and Δ_M^0 are superhorizon size, and their amplitudes are “frozen” to constants outside the horizon. With respect to the subhorizon observer, it means that $\bar{\delta}_M$ (5.7) does not vanish and the particle-antiparticle symmetry breaks in the pre-inflation and inflation epoch ($a < a_{\text{end}}$). It is the case corresponding to the super-horizon case (b) below Eq. (3.25).

6.2 Particle-antiparticle symmetry in massive pair episode

In the \mathcal{M} -episode $H < \Gamma_M/2$ and $\epsilon \approx 3/2$, when $7 \cdot 10^{-2} \lesssim \ln(a/a_{\text{end}}) \lesssim 3.6$ of Figs. 2, 3 (a) and (b), we find that the modes δ_M^0 and Δ_M^0 are inside the horizon. This is because the the ratio of horizon radius and pair oscillating length is larger than 2,

$$\frac{H^{-1}}{\omega_\delta^{-1}} = \left(\frac{H^{-2}}{2^{-1}H^{-1}\Gamma_M^{-1}} \right)^{1/2} > \left(\frac{2\Gamma_M^{-1}}{2^{-1}\Gamma_M^{-1}} \right)^{1/2} = 2. \quad (6.2)$$

It means that the modes δ_M^0 and Δ_M^0 are subhorizon sized and underdamped oscillations, corresponding to the underdamped case ($\zeta < 1$). We use the numerical results in Ref. [48] to show the ratio (6.2) in Fig. 3 (a), where the blue line $H^{-1}/\omega_\delta^{-1}$ is above the orange line 2. Therefore, in the \mathcal{M} -episode the particle-antiparticle asymmetric mode δ_M^0 and symmetric mode Δ_M^0 are well inside the horizon. They behave as underdamped oscillating waves whose dampened amplitudes vanish within the horizon H^{-1} . Their root-mean-square density fluctuations (5.1) $\bar{\delta}_M = 0$ and $\bar{\Delta}_M = 0$ vanish. It means that with respect to the subhorizon observer, the asymmetric perturbation (5.7) vanishes and the particle-antiparticle symmetry holds in the \mathcal{M} -episode.

The $\bar{\delta}_M = 0$ and $\bar{\Delta}_M = 0$ equivalently correspond to the averaged $\langle \delta_M^0 \rangle = 0$ and $\langle \Delta_M^0 \rangle = 0$ over the Hubble time scale $\tau_H \sim H^{-1}$, which is larger than the perturbation time scale τ_M (2.3). The $\langle \Delta_M^0 \rangle = 0$ corresponds to the detailed balance of perturbations $\rho_M^\pm \Leftrightarrow \rho_M^H/2$ in the rate equation (3.1) inside the horizon. Therefore, the net number of particles and antiparticles is zero and the particle-antiparticle symmetry is preserved in the \mathcal{M} -episode.

6.3 Subhorizon crossing point in pre-reheating episode

Form the superhorizon size (6.1) in the pre-inflation and inflation epoch to the subhorizon size (6.2) in the \mathcal{M} -episode, the modes δ_M and Δ_M cross at least once the horizon. Because the H and Γ_M vary monotonically, Equations (6.1) and (6.2) show that one horizon crossing point $\omega_\delta = H$ locates at $H = \Gamma_M/2$ in the pre-reheating \mathcal{P} -episode, when $10^{-3} \lesssim \ln(a/a_{\text{end}}) \lesssim 7 \cdot 10^{-2}$ of Figs. 2, 3 (a) and (b). Using Eq. (4.4), we find the subhorizon crossing scale H_{crin} and oscillating frequency $\omega_\delta^{\text{crin}}$ at the horizon-crossing scale factor a_{crin} ,

$$H_{\text{crin}} = \Gamma_M/2 \approx H_{\text{end}}/2, \quad \omega_\delta^{\text{crin}} = (2\Gamma_M H)^{1/2} \approx H_{\text{end}}, \quad (6.3)$$

which are the same order of the inflation end scale $H_{\text{end}} \approx \Gamma_M$. In Fig. 3 (a), using previous numerical results, we plot the ratio $H^{-1}/\omega_\delta^{-1} = (2\Gamma_M/H)^{1/2}$ (6.2), starting from the inflation end H_{end} , to show the subhorizon crossing occurs at $x = \ln(a_{\text{crin}}/a_{\text{end}}) \approx 5 \times 10^{-3}$, i.e., $a_{\text{crin}} \approx 1.01a_{\text{end}}$ in the preheating \mathcal{P} -episode. It shows that the subhorizon crossing occurs right after the inflation end, $H_{\text{crin}} > H_{\text{end}}$ and $a_{\text{crin}} \gtrsim a_{\text{end}}$.

In the pre-inflation and inflation epoch, the subhorizon observer views the particle-antiparticle asymmetry because some of the particles or antiparticles are outside the horizon. These superhorizon particle or antiparticle modes cross back to the horizon in the \mathcal{P} -episode. The subhorizon observer views the particle-antiparticle symmetry in the \mathcal{M} -episode because all particles and antiparticles are inside the horizon. At such subhorizon crossing a_{crin} , the number of particles or antiparticles can be calculated as follows. The numerical value $\epsilon_{\text{cr}} = \epsilon_{\text{crin}} \approx 1.0 \times 10^{-2}$ at the subhorizon crossing a_{crin} can be found from Fig. 2 and 3 (a). We use Eq. (5.6) to calculate the asymmetric and symmetric pair density perturbations

$$\bar{\delta}_M^{\text{crin}} = \bar{\Delta}_M^{\text{crin}} \approx 4.33 \times 10^{-6}, \quad (6.4)$$

at the subhorizon crossing a_{crin} . Then the net particle density perturbation (5.7) and the pair density perturbation (5.8) at the subhorizon crossing (6.3) are given by,

$$\rho_M^+ - \rho_M^- = \bar{\delta}_M^{\text{crin}} \rho_M^H \approx \bar{\delta}_M^{\text{crin}} (\hat{m}^2 H_{\text{end}}^2)/2, \quad (6.5)$$

$$\rho_M - \rho_M^H = \bar{\Delta}_M^{\text{crin}} \rho_M^H \approx \bar{\Delta}_M^{\text{crin}} (\hat{m}^2 H_{\text{end}}^2)/2. \quad (6.6)$$

They are about 10^{-3} in unit of the characteristic density $\rho_{\text{end}}^c = 3m_{\text{pl}}H_{\text{end}}^2$ at inflation end. The particle-antiparticle asymmetry (6.5) is on the horizon surface at the subhorizon crossing. It represents the superhorizon particle-antiparticle asymmetry in the pre-inflation and inflation epochs. It also represents the subhorizon restoration of the particle-antiparticle symmetry in the \mathcal{M} -episode. This is because the total number of particles and antiparticles inside and outside the horizon is zero.

As shown in Fig. 3 (a), after the subhorizon crossing (6.3), the subhorizon sized modes δ_M^0 and Δ_M^0 remain inside the horizon as underdamped oscillating modes in the \mathcal{M} -episode and preserve particle and antiparticle symmetry, until they undergo the superhorizon crossing in the genuine reheating \mathcal{R} -episode.

7 Superhorizon crossing in genuine reheating

We will show the modes δ_M^0 and Δ_M^0 superhorizon crossing in the transition period from the massive pair domination \mathcal{M} -episode to the genuine reheating \mathcal{R} -episode when unstable massive pairs predominately decay into relativistic particles (w.r.t the reheating temperature) in the SM and dark matter particle contents. Such a superhorizon crossing produces particle-antiparticle asymmetry, giving rise to an initial condition for the standard cosmology after the reheating.

7.1 Superhorizon crossing point in massive pair episode

In the genuine reheating \mathcal{R} -episode, the horizon scale H is mainly determined by unstable pairs' decay since the pair decay rate Γ_M^{de} (time τ_R) is much larger (shorter) than the rate Γ_M (time τ_M) of massive pair perturbations. In Eq. (3.1), the decay term $\Gamma_M^{\text{de}} \rho_M^\pm$ is dominant, and the density perturbations $\rho_M^\pm \Leftrightarrow \rho_M^0$ are no longer relevant. Unstable massive pairs rapidly decay to relativistic particles.

We adopt the horizon size H^{-1} approximately determined by the reheating scale H_{RH} at the scale factor a_R ,

$$H_{\text{RH}}^2 = (2\tau_R)^{-2} = (\Gamma_M^{\text{de}}/2)^2, \quad (7.1)$$

which is the first equation in (5.74) of Ref. [58] and Eq. (7.31) of Ref. [48]. To examine the modes δ_M^0 and Δ_M^0 are subhorizon size or superhorizon size in the \mathcal{R} -episode, we use the criteria (4.4) or (4.5),

$$\frac{H^{-1}}{\omega_\delta^{-1}} = \left(\frac{2\Gamma_M}{H} \right)^{1/2} \approx 2(\tau_R \Gamma_M)^{1/2} = 2 \left(\frac{\Gamma_M}{\Gamma_M^{\text{de}}} \right)^{1/2} < 2. \quad (7.2)$$

The last inequality or $\Gamma_M < 2H_{\text{RH}} \approx \Gamma_M^{\text{de}}$ shows that the modes δ_M^0 and Δ_M^0 are superhorizon sizes in the \mathcal{R} -episode.

From the subhorizon-sized modes in the \mathcal{M} -episode to the superhorizon-sized modes in the \mathcal{R} -episode, the δ_M^0 and Δ_M^0 modes' superhorizon crossing must occur in the transition period from the \mathcal{M} -episode to the \mathcal{R} -episode. The superhorizon crossing occurs at $H_{\text{crou}}^{-1}/\omega_\delta^{-1} = 2$, yielding

$$H_{\text{crou}} = \Gamma_M^{\text{crou}}/2 \approx \Gamma_M^{\text{de}}/2, \quad \Gamma_M^{\text{crou}} \approx \Gamma_M^{\text{de}}, \quad (7.3)$$

consistently with the horizon crossing condition (4.4) or (4.5). The approximation $\Gamma_M^{\text{crou}} \approx \Gamma_M^{\text{de}}$ comes from $H_{\text{crou}} \approx H_{\text{RH}} = (\Gamma_M^{\text{de}}/2)$. It implies that the superhorizon crossing occurs at

$$H_{\text{crou}} \gtrsim H_{\text{RH}}, \quad a_{\text{crou}} \lesssim a_R, \quad (7.4)$$

near to the reheating scale H_{RH} and a_R .

To verify such a superhorizon crossing point (7.3), we use previous numerical results to plot the ratio $H^{-1}/\omega_\delta^{-1} \approx 2\tau_R/\tau_M$ of the horizon radius and the δ_M^0 mode oscillating length in Fig. 3 (b). It shows that the ratio $H^{-1}/\omega_\delta^{-1}$ (blue line) varies from subhorizon (> 2) to superhorizon (< 2). The superhorizon crossing H_{crou} and a_{crou} (7.4) are at the \mathcal{M} -episode end, which are indeed close to the genuine reheating H_{RH} and a_R (7.1).

7.2 Particle-antiparticle asymmetry occurs in reheating epoch

As illustrated in Figs. 3 (b), the modes δ_M^0 and Δ_M^0 have the superhorizon crossing (7.4) in the genuine reheating \mathcal{R} -episode. The subhorizon observer views:

- (i) the particle and antiparticle symmetry in the massive pair \mathcal{M} -episode;
- (ii) superhorizon crossing (7.4) produces the particle and antiparticle asymmetry in the genuine reheating \mathcal{R} -episode.

Due to the superhorizon crossing at $a_{\text{crou}} \lesssim a_R$, the δ_M^0 is an overdamped oscillating mode frozen outside the horizon, its root-mean-squared (*rms*) value $\bar{\delta}_M$ does not vanish. It indicates that some particle (or anti-particle) modes are frozen outside the horizon. From Eq. (5.6), we obtain the asymmetric and symmetric pair density perturbations at the superhorizon crossing (7.3)

$$\bar{\delta}_M^{\text{crou}} = \bar{\Delta}_M^{\text{crou}} = 2.31 \times 10^{-4}, \quad (7.5)$$

by using $\epsilon_{\text{cr}} = \epsilon_{\text{crou}} \approx 2$ in the genuine reheating \mathcal{R} -episode. Based on Eq. (5.7), we calculate the particle-antiparticle asymmetric number density, i.e., the net number density of particles and antiparticles,

$$\delta n_M^{\text{crou}} = \frac{\rho_M^+ - \rho_M^-}{2\hat{m}} = \bar{\delta}_M^{\text{crou}} n_M^H|_{\text{crou}}, \quad (7.6)$$

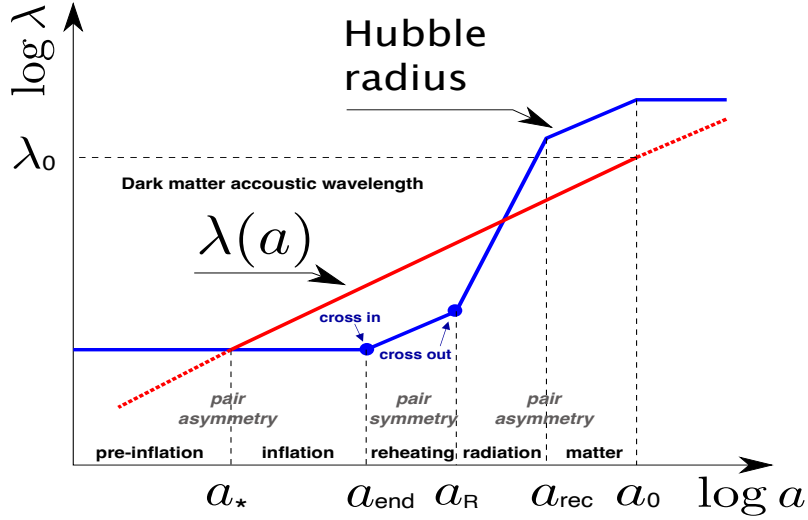


Figure 4. We make this figure by modifying Fig. 1 in Ref. [66] to illustrate schematic evolution of the Hubble radius H^{-1} and the physical wavelength $\lambda(a)$ of dark matter acoustic wave. The wavelength $\lambda_0 = \lambda(a_0)$ at the present time $a_0 = 1$ crossed the Hubble horizon H_* at the early time a_* , fixed by the physically interesting length scale $\lambda_0 = \lambda_* = k_*^{-1}$. The pre-inflation $a > a_*$, the inflation $a_* < a < a_{\text{end}}$, the reheating $a_{\text{end}} < a < a_R$, and the recombination at a_{rec} . The subhorizon “cross in” point corresponds to the point in Fig. 3 (a). The superhorizon “cross out” point corresponds to the point in Fig. 3 (b).

at the superhorizon crossing $H_{\text{crou}} \gtrsim H_{\text{RH}}$ and $a_{\text{crou}} \lesssim a_R$. As a result, we approximately obtain the net number density of particles and antiparticles,

$$\delta n_M^{\text{crou}} = \frac{\rho_M^+ - \rho_M^-}{2\hat{m}} \Big|_{\text{crou}} \approx 2.31 \times 10^{-4} n_M^H \Big|_{\text{crou}}, \quad (7.7)$$

and $n_M^H \Big|_{\text{crou}} \approx \chi \hat{m} H_{\text{RH}}^2$. Analogously, we obtain from Eq. (5.8) the pair number density perturbation of massive particles,

$$\Delta n_M^{\text{crou}} = \frac{\rho_M - \rho_M^H}{2\hat{m}} \Big|_{\text{crou}} \approx 2.31 \times 10^{-4} n_M^H \Big|_{\text{crou}}. \quad (7.8)$$

The asymmetric modes δ_M^0 carried the net particle number has been frozen in the superhorizon.

It is important to note that the total number of particles and antiparticles inside and outside the horizon is zero and preserved. The positive (negative) net number of particles and antiparticles inside the horizon is equal to the negative (positive) net number of particles and antiparticles outside the horizon. The latter is described by the asymmetric perturbation $\bar{\delta}_M$ on the surface of the superhorizon crossing (7.5).

To illustrate our discussions, we schematically show in Fig. 4 the particle-antiparticle pair symmetry and asymmetry in different epochs and indicate the occurrences of subhorizon cross-in and superhorizon cross-out. At the end of \mathcal{M} -episode of reheating, a tiny asymmetry (7.7) of massive particles and antiparticles appears inside the horizon.

Such a nonzero net number of massive particles and antiparticles inside the horizon is preserved during the entire history of standard cosmology, since superhorizon criteria $H^{-1}/\omega_{\delta}^{-1} = (2\Gamma_M/H)^{1/2} < 2$ (7.2) and $H > \Gamma_M$ holds after reheating.

8 Baryogenesis in reheating epoch

We will show that the asymmetry of massive particles X and antiparticles \bar{X} of the net number density (7.7) results in the asymmetry of baryon numbers of baryons B and antibaryons \bar{B} at the reheating end, which leads to baryogenesis in agreement with observations.

8.1 Initial baryon asymmetry for standard cosmology

In the reheating \mathcal{R} -episode after the superhorizon crossing (7.4), unstable massive pairs rapidly decay into relativistic particles, and the final states are gauge bosons, leptons and baryons in the SM and dark matter particles. Massive pair decay process $\bar{X}X \Rightarrow \bar{\ell}\ell$ and all other microscopic processes respect the CPT symmetry and other fundamental symmetries. The asymmetry (7.7) of massive particles X and antiparticles \bar{X} leads to the asymmetry between baryons and anti-baryons, the asymmetry between leptons and anti-leptons, and the asymmetry between dark-matter particles and antiparticles. These SM and dark-matter particle-antiparticle asymmetries are initial conditions for starting standard cosmology. The asymmetry (7.7) of X and \bar{X} also accounts for dark-matter particle and anti-particle asymmetry in the present Universe.

Such a scenario sharply contrasts with the usual dynamic scenarios that initial particles X and antiparticles \bar{X} compositions are symmetric. The production of baryon B and anti-baryon \bar{B} asymmetry requires the interactions between \bar{X}, X and \bar{B}, B obey three Sakharov conditions that B - and CP -violating X decays to baryons B and decouples from thermal equilibrium in cosmic evolution, as discussed in the introduction. The particles X and antiparticles \bar{X} asymmetry (7.4) created by the superhorizon crossing (7.7) acts as an explicit CP -symmetry breaking between particles X and antiparticles \bar{X} in either their effective Lagrangian or their initial condition of compositions, which persists in standard cosmology after the reheating. This article will focus only on the resultant asymmetry between the baryon and anti-baryon. The lepton-antilepton and dark-matter particle-antiparticle asymmetries will be issues for future studies.

8.2 Net baryon numbers and baryon number-to-entropy ratio

Following the approach discussed in Ref. [58], we use the net particle number density $\delta n_M^{\text{crou}}(7.7)$ and the continuity equation of the net baryon number density n_B to obtain

$$\begin{aligned} \dot{n}_B + 3Hn_B &= \delta n_M^{\text{crou}}/\tau_R, \\ \Rightarrow n_B(a) &= 2.31 \times 10^{-4} n_M^H(a_R) \left(\frac{a}{a_R}\right)^{-3} [1 - \exp -t/\tau_R]. \end{aligned} \quad (8.1)$$

Note that the net number density $\delta n_M^{\text{crou}} (7.7)$ of massive particles and antiparticles is the counterpart of mean net baryon number density $\epsilon_{\text{CP}} n_B$ in Ref. [58], attributing to an explicit CP -symmetry violating interaction in an effective Lagrangian. There, massive particles X and antiparticles \bar{X} CP -violating decays produce a mean net baryon number $\epsilon_{\text{CP}} n_B$. Here, the superhorizon crossing of massive particles and antiparticles oscillating mode leads to the net number density $\delta n_M^{\text{crou}} (7.7)$. Via massive particles' decay to baryons, the net number density δn_M^{crou} leads to a net baryon number density in the right-handed side of the continuity equation (8.1).

In the second line of integration, the initial moment $t_i \ll \tau_R$ is assumed and the solution for massive pairs ρ_M decay is used, see Eq. (7.23) of Ref. [48] or the first equation in (6.61) of Ref. [58]. The physical content is clear: at late times, $t \gg \tau_R$, the net baryon number per comoving volume $a^3 n_B(a)$ is just 2.31×10^{-4} times the initial number of massive particles per comoving volume $a_R^3 n_M^H(a_R)$. Note that $a^3 n_B(a)$ is the comoving number density, whereas $n_B(a)$ is the physical number density, i.e., the net baryon number per physical volume. Since the decay time scale $\tau_R \propto \hat{m}^{-1}$ is very short, we adopt the approximation that the superhorizon crossing coincides with the genuine reheating (7.4) ($a = a_R \approx a_{\text{crou}}$ and $t \approx \tau_R$) to obtain the net baryon number density

$$n_B^R(a_R) = 1.46 \times 10^{-4} n_M^H(a_R), \quad n_M^H(a_R) = \chi \hat{m} H_{\text{RH}}^2. \quad (8.2)$$

It yields the origin of the net number of baryons or antibaryons, i.e., the baryogenesis in the Universe.

As a CP -asymmetric relic from the reheating epoch or as a CP -initial asymmetric state of the standard cosmology, the CP -asymmetry persists after the reheating. The net baryon number (8.2) remains inside the horizon and conserves in subsequent Universe evolution. It accounts for the baryon and anti-baryon asymmetry observed today. It should be emphasized that in our scenario, the standard cosmology starts from the initial state of asymmetrical baryon and antibaryon numbers. Therefore the three Sakharov conditions [28] of dynamical solution for the baryogenesis are not applicable.

Using the entropy S_R and temperature T_{RH} of the reheating epoch, obtained in Eqs. (8.6) and (8.8) of Ref. [48], we calculate the baryon asymmetry represented by the ratio of the net baryon number $a_R^3 n_B^R$ (8.2) to the entropy S_R . Per comoving volume, this ratio at the reheating a_R is given by

$$\frac{n_B^R}{s_R} = \frac{a_R^3 n_B^R}{S_R} \approx 1.46 \times 10^{-4} \frac{a_R^3 n_M^H(a_R)}{S_R} \approx 2.6 \times 10^{-4} \frac{T_{\text{RH}}}{\hat{m}}, \quad (8.3)$$

where the entropy density $s_R = S_R/a_R^3$ at the genuine reheating \mathcal{R} -episode. This result is consistent with the one derived from the processes of baryon-number violating decay in Ref. [58]. This baryon number-to-entropy ratio n_B^R/s_R (8.3) preserves its value from the reheating epoch to the present time. The present observational value is $n_B/s = 0.864_{-0.015}^{+0.016} \times 10^{-10}$ [27]. This determines the ratio of the reheating temperature T_{RH} to the mass parameter \hat{m} ,

$$(T_{\text{RH}}/\hat{m}) \approx 3.3 \times 10^{-7}. \quad (8.4)$$

It is used to constrain the parameters $(g_Y^2/g_*^{1/2})$ and (\hat{m}/M_{pl}) , see Eq. (8.11) of Ref. [48], g_* is the effective degeneracy of SM light particles $\bar{\ell}\ell$ produced in reheating.

In this article, we determine the ratio of parameters (8.4) by considering the observed baryogenesis resulting from the asymmetry of particles X and antiparticles \bar{X} due to the horizon-crossing dynamics in the reheating epoch. Such an asymmetry can also cause SM leptogenesis and the asymmetry between sterile dark matter particles and antiparticles because particles X and antiparticles \bar{X} can annihilate and decay to SM leptons and dark matter particles. The ratio (8.4) will be better constrained if leptogenesis and asymmetries of sterile dark matter particles and antiparticles are determined. These are subjects for future studies.

9 Dark-matter acoustic wave and large-scale structure

We describe in Sec. 3 the density perturbation modes $\delta_M^{\mathbf{k}}$ and $\Delta_M^{\mathbf{k}}$ of massive particle-antiparticle pair plasma. We focus on the “zero mode” $|\mathbf{k}| = 0$ oscillating modes δ_M^0 and Δ_M^0 of the frequency $\omega = (2H\Gamma)^{1/2}$ in Sec. 4. We study their subhorizon crossing in Sec. 6 and superhorizon crossing in Sec. 7. The latter accounts for the baryogenesis in Sec. 8.

From this section, we will study wave-propagating modes $\delta_M^{\mathbf{k}}$ and $\Delta_M^{\mathbf{k}}$ ($|\mathbf{k}| \neq 0$) of the frequencies $\omega_{\delta,\Delta}(|\mathbf{k}|)$ (3.20) and (3.21). They represent dark-matter acoustic waves, as indicated by the red line in Fig. 4, that exited from (superhorizon crossing out) the horizon and reentered into (subhorizon crossing in) the horizon again. In particular, we focus on the pair symmetric density perturbation modes $\Delta_M^{\mathbf{k}}$. We examine the negative term $4\pi G\rho_M^H\Delta_M^{\mathbf{k}}$ in the frequency $\omega_{\Delta}(|\mathbf{k}|)$ (3.21) to study the Jeans instability for the cases: (a) the pre-inflationary epoch where the mass parameter $m \gtrsim H$ and $v_s^2 \lesssim 1$, namely, pairs can be relativistic; (b) the inflationary epoch where the mass parameter $m \gg H$ and $v_s^2 \ll 1$, namely pairs are non-relativistic. Here the mass parameter m are the values for the pre-inflation or inflation epoch. To be specific, we investigate the wave-propagating modes $\Delta_M^{\mathbf{k}}$ and $\delta_M^{\mathbf{k}}$:

- (i) in the pre-inflation and inflation epochs, their superhorizon crossings out and modes frozen or amplified outside of the horizon;
- (ii) after the recombination, their subhorizon crossings reentry the horizon, yielding peculiar “dark-matter” acoustic waves imprinting on the matter power spectrum at large length scales;
- (iii) their possible impacts on forming large-scale structures and galaxy profiles.

To start with, we would like to emphasize that the perturbations discussed here are the kinds of acoustic waves of the dispersion relations (3.20) and (3.21). They are due to fluctuations in the form of the local equation of the state $\omega_M = v_s^2$ (3.11) of particles and antiparticles, namely, spatial fluctuations in the number of particles or antiparticles (compositions) per comoving volume. Its physical nature differs from the curvature perturbations as fluctuations in energy density characterized by the local value of the spatial curvature of the spacetime.

9.1 Wave modes, horizon crossings, and Jeans instability

The wave modes are described by the comoving momentum $|\mathbf{k}|$ (wavelength $\lambda = |\mathbf{k}|^{-1}$), whose value is constant in time. As a reference, we consider the pivot scale $k^* = 0.05(\text{Mpc})^{-1}$, at which the curvature perturbations cross outside and inside horizons twice, accounting for the CMB observations. The corresponding values of the horizon $k^* = (Ha)_*$, the ϵ -rate $\epsilon = \epsilon^*$ and the mass parameter $m = m_*$ for inflation, that are given in Sec. 6 of Ref. [47] or [48].

The case $|\mathbf{k}| > k^*$ corresponds to the wave modes that exit the horizon in the pre-inflation epoch and reenter the horizon after the recombination epoch. The case $|\mathbf{k}| < k^*$ corresponds to the wave modes that exit the horizon in the inflation epoch and reenter the horizon before the recombination epoch. In both cases, $H \gg \Gamma_M = (\chi/4\pi)m\epsilon$ and $\epsilon \ll 1$. Wave equations (3.18) and (3.19) approximately become,

$$\ddot{\delta}_M^{\mathbf{k}} + 2H\dot{\delta}_M^{\mathbf{k}} \approx -\omega_\delta^2(|\mathbf{k}|)\delta_M^{\mathbf{k}}, \quad (9.1)$$

$$\ddot{\Delta}_M^{\mathbf{k}} + 2H\dot{\Delta}_M^{\mathbf{k}} \approx -\omega_\Delta^2(|\mathbf{k}|)\Delta_M^{\mathbf{k}}, \quad (9.2)$$

where the Hubble rate H slowly varies $H \approx \text{const}$. Following the same discussions in previous Sec. 4 or the usual discussions of the curvature perturbations, these wave modes $\delta_M^{\mathbf{k}}$ and $\Delta_M^{\mathbf{k}}$ superhorizon crossing at a^* when $\omega_{\delta,\Delta}(|\mathbf{k}|) = 2H$ (4.5), see Fig. 4. We use the frequencies $\omega_{\delta,\Delta}(|\mathbf{k}|)$ (3.20) and (3.21) to obtain the wavenumber $|\mathbf{k}|_{\delta,\Delta}$ at the superhorizon crossing,

$$|\mathbf{k}|_{\delta\text{cross}}^2 = \left(4 - \chi \frac{\epsilon m}{2\pi H}\right) \frac{(Ha)^2}{v_s^2} \Big|_{\text{cross}} \approx 4 \frac{(Ha)^2}{v_s^2} \Big|_{\text{cross}}, \quad (9.3)$$

$$\begin{aligned} |\mathbf{k}|_{\Delta\text{cross}}^2 &= \left[4 - \chi \frac{\epsilon m}{2\pi H} + \chi \left(\frac{m}{m_{\text{pl}}}\right)^2\right] \frac{(Ha)^2}{v_s^2} \Big|_{\text{cross}} \\ &\approx 4 \frac{(Ha)^2}{v_s^2} \Big|_{\text{cross}} \approx |\mathbf{k}|_{\delta\text{cross}}^2. \end{aligned} \quad (9.4)$$

The sound velocity v_s value (3.11) decreases from the relativistic case $v_s \lesssim 1$ (pre-inflation $m \gtrsim H$) to the non-relativistic case $v_s \ll 1$ (inflation $m \gg H$), as the horizon H decreases and the equation of state $p_M^H = \omega_M^H \rho_M^H$ (2.2) changes from $\omega_M^H \lesssim 1/3$ to $\omega_M^H \approx 0$ [47, 56].

The horizon crossing (9.3) and (9.4) shows that because of $v_s^2 < 1$, the modes $|\mathbf{k}|_{\delta\text{cross}, \Delta\text{cross}} > k^*$ cross the horizon before the inflation pivot scale $k^* = (Ha)_*$, and reenter the horizon after the recombination $(Ha)_*$. Therefore, these acoustic wave perturbations can cross to outside the horizon in the pre-inflation epoch and then cross inside the horizon after the recombination. The acoustic wave modes of larger $|\mathbf{k}|_{\delta\text{cross}, \Delta\text{cross}}$ exit the horizon earlier and reenter the horizon later. They should leave their imprints on the linear regime of large-scale structure and the nonlinear regime of galaxy clustering. We called these acoustic or quantum wave modes of “dark-matter” waves [47, 56], and will discuss them in detail below.

The particle-antiparticle symmetric modes $\Delta_M^{\mathbf{k}}$ (3.13) represent the acoustic waves of pair-density perturbations of the dispersion relation (3.21). It is analogous to the

matter density perturbation wave in gravitation fields. We examine the dispersion relation (3.21) to check whether the Jeans instability occurs and the $\Delta_M^{\mathbf{k}}$ amplitudes amplify for imaginary frequencies $\omega_\Delta^2(|\mathbf{k}|) < 0$, i.e.,

$$|\mathbf{k}|_\Delta^2 < |\mathbf{k}|_{\text{Jeans}}^2 \equiv \chi \left[\left(\frac{m}{m_{\text{pl}}} \right)^2 - \frac{\epsilon m}{2\pi H} \right] \frac{(Ha)^2}{v_s^2}. \quad (9.5)$$

The $\omega_\Delta^2(|\mathbf{k}|) = 0$ gives the Jeans wavenumber $|\mathbf{k}|_{\text{Jeans}}$ and wavelength $\lambda_{\text{Jeans}} = |\mathbf{k}|_{\text{Jeans}}^{-1}$. The modes $\Delta_M^{\mathbf{k}}$ of wavelengths $\lambda > \lambda_{\text{Jeans}}$ undergo the Jeans instability because the gravitational attraction of pair-density perturbations prevails.

In the inflation epoch, the gravitational attractive term $4\pi G\rho_M^H$ is negligible compared with the “quasi mass” term $2H\Gamma_M$ in the frequency ω_Δ^2 (3.21). Thus $\omega_\Delta^2 > 0$ and the Jeans instability does not occur. In the pre-inflation epoch, the term $2H\Gamma_M$ is negligible compared with the gravitational attractive term $4\pi G\rho_M^H$. It is then possible to have the imaginary frequency (3.20) $\omega_\Delta^2 < 0$ for $|\mathbf{k}|_\Delta^2 < |\mathbf{k}|_{\text{Jeans}}^2$ (9.5), and

$$|\mathbf{k}|_{\text{Jeans}}^2 \approx \chi \left(\frac{m}{m_{\text{pl}}} \right)^2 \frac{(Ha)^2}{v_s^2}; \quad \chi \left(\frac{m}{m_{\text{pl}}} \right)^2 < 1, \quad (9.6)$$

where the Jeans instability occurs.

9.1.1 Subhorizon stable modes and dark-matter acoustic waves

For short-wavelength modes $|\mathbf{k}|_\Delta^2 > |\mathbf{k}|_{\text{Jeans}}^2$, the pressure terms $(v_s^2|\mathbf{k}|^2/a^2)$ are dominant in the frequency ω_Δ^2 (3.21), compared with the gravitational attraction $4\pi G\rho_M^H$ of pair-density perturbations. Equation (9.2) for the pair-density perturbation approximately becomes

$$\ddot{\Delta}_M^{\mathbf{k}} + 2H\dot{\Delta}_M^{\mathbf{k}} = -(v_s^2|\mathbf{k}|^2/a^2)\Delta_M^{\mathbf{k}}, \quad (9.7)$$

which is the typical Mukhanov-Sasaki equation, similar to the one for the curvature perturbation. Using Eqs. (4.1), (4.2) and (4.3), we find its solution

$$\Delta_M^{\mathbf{k}}(t) \propto e^{-Ht} \exp -i\tilde{\omega}_\Delta(|\mathbf{k}|)(1 - \zeta^2)^{1/2}t, \quad \zeta \approx \frac{H}{\tilde{\omega}_\Delta(|\mathbf{k}|)} = \frac{Ha}{v_s|\mathbf{k}|_\Delta}, \quad (9.8)$$

where the acoustic wave frequency $\tilde{\omega}_\Delta(|\mathbf{k}|) = v_s|\mathbf{k}|_\Delta/a$.

For given comoving horizon (Ha) and sound velocity v_s , horizon crossing wavenumber $|\mathbf{k}|_{\Delta\text{cross}} = 2Ha/v_s$ (9.4) is larger than Jeans wavenumber $|\mathbf{k}|_{\text{Jeans}}$ (9.6),

$$|\mathbf{k}|_{\Delta\text{cross}} > |\mathbf{k}|_{\text{Jeans}}. \quad (9.9)$$

This shows that the pair-density perturbations $\Delta_M^{\mathbf{k}}$ oscillate as

- (i) *sub-horizon sized modes*: an underdamped acoustic wave inside the horizon for $\zeta < 1$ and $|\mathbf{k}|_\Delta > |\mathbf{k}|_{\Delta\text{cross}} > |\mathbf{k}|_{\text{Jeans}}$. The modes $\Delta_M^{\mathbf{k}}(t)$ are stable acoustic waves;
- (ii) *super-horizon sized modes*: an overdamped acoustic wave outside the horizon for $\zeta > 1$ and $|\mathbf{k}|_{\Delta\text{cross}} > |\mathbf{k}|_\Delta > |\mathbf{k}|_{\text{Jeans}}$. The mode amplitudes $\Delta_M^{\mathbf{k}} \propto \text{const}$ are frozen.

On the other hand, as the comoving horizon (Ha) increases and the sound velocity v_s decreases in the pre-inflation and inflation epochs, the horizon crossing wavenumber $|\mathbf{k}|_{\Delta\text{cross}}$ (9.4) increases. The acoustic wave modes $\Delta_M^{\mathbf{k}}$ of fixed wavenumber $|\mathbf{k}|_{\Delta}$ evolve from *subhorizon* to *superhorizon*, and the horizon crossing occurs at $|\mathbf{k}|_{\Delta} = |\mathbf{k}|_{\Delta\text{cross}}$.

Moreover, the *super-horizon sized mode* $|\mathbf{k}|_{\Delta}$ reenters the horizon at $(Ha)_{\text{reenter}}$ and becomes a *sub-horizon sized mode*, when

$$|\mathbf{k}|_{\Delta} = (Ha)_{\text{reenter}}, \quad (9.10)$$

where $(Ha)_{\text{reenter}}^{-1}$ is the comoving horizon size after the recombination. Such mode $|\mathbf{k}|_{\Delta} = (Ha)_{\text{reenter}}$ behaves as an acoustic wave of dark-matter density perturbations. It imprints on the matter power spectrum of low- ℓ multipoles $\ell \leq 2$, corresponding to large length scales. It is reminiscent of baryon acoustic oscillations due to the coupling in the baryon-photon fluid.

These are qualitative discussions on dark-matter acoustic waves, possibly relevant for observations. However, the quantitative results depend not only on the initial amplitude value $\Delta_M^{\mathbf{k}}(0)$, the wavenumber $|\mathbf{k}|_{\Delta}$ and the horizon crossing size $(Ha)_{\text{cross}}$, but also on the sound velocity v_s in Eq. (9.8).

9.1.2 Unstable superhorizon modes and large-scale structure

For long-wavelength modes $|\mathbf{k}|_{\Delta}^2 \ll |\mathbf{k}|_{\text{Jeans}}^2$, the pressure terms $(v_s^2|\mathbf{k}|^2/a^2)$ are negligible in the frequency ω_{Δ}^2 (3.21), compared with the gravitational attraction $4\pi G\rho_M^H$ of pair-density perturbations. Equation (9.2) for the pair-density perturbation approximately becomes

$$\ddot{\Delta}_M^{\mathbf{k}} + 2H\dot{\Delta}_M^{\mathbf{k}} = \chi\left(\frac{m}{m_{\text{pl}}}\right)^2 H^2 \Delta_M^{\mathbf{k}}, \quad (9.11)$$

as the microscopic physics (e.g., pressure terms $(v_s^2|\mathbf{k}|^2/a^2)$) is impotent and negligible. The Hubble rate H is approximately a constant, slowly varies in the pre-inflation and inflation epochs.

Equation (9.11) is a new kind of differential equation for density perturbations, differently from Eq. (9.7) of the Mukhanov-Sasaki type. This equation (9.11) has two independent solutions:

$$\Delta_M^{\mathbf{k}}(t) \propto \exp -2Ht; \quad \Delta_M^{\mathbf{k}}(t) \propto \exp + \frac{\chi H}{2} \left(\frac{m}{m_{\text{pl}}}\right)^2 t. \quad (9.12)$$

At late times, the exponentially glowing modes of pair-density perturbations are crucial. Whereas the exponentially decaying modes physically correspond to those modes with initial overdensity and velocity arranged so that the initial velocity perturbation eventually eases pair-density perturbations.

Equation (9.6) shows that $|\mathbf{k}|_{\Delta}^2 \ll |\mathbf{k}|_{\text{Jeans}}^2$ means $|\mathbf{k}|_{\Delta}^2 < |\mathbf{k}|_{\Delta\text{cross}}^2$, indicating these modes (9.12) are superhorizon size. It is consistent with neglecting the pressure term $(v_s^2|\mathbf{k}|^2/a^2)$ of the microscopic physics that cannot causally arrange the pair-density perturbations in superhorizon size. As a result, the pressure terms do not balance

the gravitational attraction, leading to an increase in the amplitudes of pair-density perturbations. These unstable and superhorizon-sized modes (9.12) exponentially grow in time. Its characteristic time scale is given by the second solution in Eq. (9.12)

$$\tau_{\Delta}^{-1} = \frac{\chi H}{2} \left(\frac{m}{m_{\text{pl}}} \right)^2. \quad (9.13)$$

These solutions (modes) differ from the superhorizon-sized modes of frozen constant amplitudes (4.3) or (9.8) for $\zeta \gg 1$.

We further study such an unstable and superhorizon-sized mode of fixed wavenumber $|\mathbf{k}|_{\Delta}$ in the range

$$|\mathbf{k}|_{\text{Jeans}} > |\mathbf{k}|_{\Delta} > k^*, \quad (9.14)$$

where $|\mathbf{k}|_{\Delta_{\text{cross}}} > |\mathbf{k}|_{\text{Jeans}}$ (9.9) and k^* is the inflation pivot scale of CMB observations. The initial amplitudes $\Delta_M^{\mathbf{k}}(0)$ of such modes (9.12) and (9.14) are very small, as the curvature perturbations. However, they could greatly amplify in the superhorizon before reentering the subhorizon. Therefore, it is possible that such modes $\Delta_M^{\mathbf{k}}$ of the pair-density perturbation are no longer a small perturbation, when they reenter the horizon and their wavelength $|\mathbf{k}|_{\Delta}^{-1}$ becomes subhorizon-sized, $|\mathbf{k}|_{\Delta} = (Ha)_{\text{reenter}}$ (9.11). The subhorizon crossing occurs after the recombination $(Ha)_{\text{reenter}} < (Ha)_*$. As a consequence, this phenomenon could play crucial physical roles in the formations of large-scale structures and galaxy cluster profiles at much larger scales.

We recall the basic scenario of primordial curvature perturbations leading to the large-scale structure in the standard cosmology. The curvature perturbations, whose amplitudes are small constants in superhorizon, reenter the horizon and lead to the CMB temperature anisotropic fluctuation $\delta T/T \sim \mathcal{O}(10^{-5})$. Such fluctuations relate to the matter density perturbations $\delta\rho/\rho \propto \delta T/T$ at the recombination of the redshift $z \sim 10^3$. These matter density perturbations (amplitudes) are small, and their physical sizes (wavelengths) increase linearly as the scale factor $a(t)$. However, under the influence of their gravitational attractions and the Jeans instability, the matter density perturbations glow $\delta\rho/\rho \propto \mathcal{O}(1)$ and become nonlinear, therefore approximately maintain constant physical sizes, eventually forming a large-scale structure.

Our qualitative analysis and discussions show the following additional possibilities. The amplitudes of unstable pair-density perturbation modes in the range (9.14) get amplification in the superhorizon up to the order of unity $\Delta_M^{\mathbf{k}} \propto \mathcal{O}(1)$, when they reenter the horizon after the recombination. Therefore, they should have some physical consequences on the formation of large-scale structures and galaxies' profiles, as well as homogeneities on scales beyond $\sim 100 Mpc/h$. However, we are not able to give quantitative results in this article and further studies are required.

9.2 Particle-antiparticle “neutral plasma” acoustic wave

We turn to the discussions of the particle-antiparticle density perturbations $\delta_M^{\mathbf{k}}$, described by the frequency $\omega_{\delta}(\mathbf{k})$ (3.20) and wave mode equation (9.1),

$$\ddot{\delta}_M^{\mathbf{k}} + 2H\dot{\delta}_M^{\mathbf{k}} = -(v_s^2|\mathbf{k}|^2/a^2)\delta_M^{\mathbf{k}}, \quad (9.15)$$

and horizon crossing (9.4). These are the same equations as those for the pair-density perturbations $\Delta_M^{\mathbf{k}}$, except the absence of the gravitational attraction term $4\pi G\rho_M^H$ and Jeans instability. The solution is similar to the stable $\Delta_M^{\mathbf{k}}$ modes (9.8)

$$\delta_M^{\mathbf{k}}(t) \propto e^{-Ht} \exp -i\tilde{\omega}_\delta(|\mathbf{k}|)(1 - \zeta^2)^{1/2}t, \quad \zeta \approx \frac{H}{\tilde{\omega}_\delta(|\mathbf{k}|)} = \frac{Ha}{v_s|\mathbf{k}|_\delta}, \quad (9.16)$$

where the acoustic wave frequency $\tilde{\omega}_\delta(|\mathbf{k}|) = v_s|\mathbf{k}|_\delta/a$. For given comoving horizon (Ha) , sound velocity v_s , and horizon crossing wavenumber $|\mathbf{k}|_{\delta\text{cross}} = 2Ha/v_s$ (9.3), the particle-antiparticle density perturbation modes $\delta_M^{\mathbf{k}}$ behave as

- (i) *sub-horizon sized modes*: an underdamped acoustic wave mode inside the horizon for $\zeta < 1$ and $|\mathbf{k}|_\delta > |\mathbf{k}|_{\delta\text{cross}}$. The modes $\delta_M^{\mathbf{k}}(t)$ are stable acoustic wave modes;
- (ii) *super-horizon sized modes*: an overdamped acoustic wave mode outside the horizon for $\zeta > 1$ and $|\mathbf{k}|_\delta < |\mathbf{k}|_{\delta\text{cross}}$. The mode amplitudes $\delta_M^{\mathbf{k}} \propto \text{const}$ are frozen.

On the other hand, as comoving horizon (Ha) increases and sound velocity v_s decreases in the pre-inflation epoch, horizon crossing wavenumber $|\mathbf{k}|_{\delta\text{cross}}$ (9.3) increases. The modes $\delta_M^{\mathbf{k}}$ of fixed wavenumber $|\mathbf{k}|_\delta$ evolve from a *sub-horizon sized mode* to a *super-horizon sized mode*, and horizon crossing occurs at $|\mathbf{k}|_\delta = |\mathbf{k}|_{\delta\text{cross}}$ (9.3). Moreover, *super-horizon sized mode* $|\mathbf{k}|_\delta$ reenters the horizon at the horizon $(Ha)_{\text{reenter}}$, when

$$|\mathbf{k}|_\delta = (Ha)_{\text{reenter}}, \quad (9.17)$$

after the recombination. It becomes a *sub-horizon sized mode* again.

The modes $|\mathbf{k}|_\delta = (Ha)_{\text{reenter}}$ of the particle-antiparticle density perturbations $\delta_M^{\mathbf{k}}$ (3.13) represent the acoustic waves of particle and antiparticle oscillations of the dispersion relation (3.20). They are analogous to the neutral plasma oscillations of electrons and positrons. They respect the symmetry of particles and antiparticles. These modes exit the horizon in the pre-inflation epoch and reenter the horizon after the recombination. It implies that such acoustic waves from the primordial Universe would leave their imprints on the Universe after the recombination. It possibly imprints on the matter power spectrum of low- ℓ multipoles $\ell \leq 2$, corresponding to large-length scales. However, we expect that the mode amplitudes $\delta_M^{\mathbf{k}}$ should be small, given the energy densities ρ_M^+ and ρ_M^- of particles and antiparticles are small. Namely, the pair energy densities $\rho_M^H \approx \rho_M^+ + \rho_M^-$ and $\rho_M^+ \approx \rho_M^-$ are small in the pre-inflation epoch.

In this section, we qualitatively describe three types of “dark-matter” acoustic waves originated from the particle-antiparticle oscillations in the pre-inflation epoch: (i) stable subhorizon pair-density perturbations; (ii) unstable superhorizon pair-density perturbations; (iii) particle-antiparticle density perturbations. We present some discussions on their returns to the horizon after the recombination and possible relevance for observations. However, we cannot give quantitative results that depend not only on perturbation modes’ wavenumbers $|\mathbf{k}|_{\Delta,\delta}$, initial amplitude values $\Delta_M^{\mathbf{k}}(0)$ and $\delta_M^{\mathbf{k}}(0)$, and sound velocity v_s in their oscillating equations (9.7) and (9.15), but also on horizon crossing size $(Ha)^{-1}$ (9.3) and (9.4). We mention that the discussions here can be applied to dark-matter waves due to the quantum fluctuation of dark-matter particles.

10 Summary and remarks

The article presents studies of particle-antiparticle asymmetry, baryogenesis and dark-matter acoustic waves in the scenario $\tilde{\Lambda}$ CDM. We summarize the lengthy article by briefly summarizing the fundamental equations adopted, basic physical phenomena described and results obtained that possibly give some insight into the issues of baryogenesis, dark matter particle-antiparticle asymmetry and large-scale structures of the Universe.

We study the perturbations of particle and antiparticle densities of massive pair plasma state in the reheating. Starting from Eqs. (3.1-3.4) for the density perturbations of particles and antiparticles, we derive the acoustic wave equations (3.18-3.19) for the particle-antiparticle symmetric pair-density perturbation Δ_M (3.12) and the particle-antiparticle asymmetric density perturbation δ_M (3.13). We study the oscillating behaviours of the lowest-lying modes of zero wavenumbers $|\mathbf{k}|_{\Delta,\delta} = 0$. We show that they evolve from superhorizon to subhorizon (6.2) in the preheating episode and from subhorizon to superhorizon (7.2) in the genuine reheating episode. In the latter case, δ_M undergoes horizon crossing to generate the net number density (7.7) of particle and antiparticle, leading to the dark-matter particle-antiparticle asymmetry and baryogenesis phenomenon. We obtain the baryon number-to-entropy ratio (8.3) consistent with observations. The δ_M measures the relative (contrast) density of particles X and antiparticles \bar{X} , whose spacetime oscillations are not in phase. This aspect is analogous to the isocurvature perturbation of the relative density of different particle species distributions, which are not in phase in spacetime. Here, we study the asymmetric perturbations δ_M , their super-horizon-crossing in the reheating epoch and never return to the horizon, which could account for the baryogenesis of the baryon number-to-entropy ratio n_B^R/s_R observed in the present Universe. As a result, the ratio (8.4) of reheating temperature T_{RH} and energy-mass scale \hat{m} is constrained. Whereas, the isocurvature perturbation from the inflation epoch is due to the perturbation of scalar field components differing from the dominant scalar-field component that drives inflation. Their return to the horizon and impact on the last-scattering epoch can be constrained by the CMB observations.

In addition, we study the acoustic wave-propagating modes ($|\mathbf{k}|_{\Delta,\delta} \neq 0$) of the pair-density perturbation $\Delta_M^{\mathbf{k}}$ (9.2) and the particle-antiparticle asymmetric density perturbation $\delta_M^{\mathbf{k}}$ (9.1). They represent the dark-matter acoustic waves. We show how they become superhorizon-sized modes (9.3) and (9.4) in the pre-inflation epoch, then return to the horizon $|\mathbf{k}|_{\Delta,\delta} = (Ha)_{\text{reenter}}$ after the recombination. These modes can behave as stable acoustic waves of dark matter density perturbations. They possibly imprint on the matter power spectrum of low- ℓ multipoles $\ell \leq 2$, corresponding to large-length scales. Due to the Jeans instability of the pair-density perturbation $\Delta_M^{\mathbf{k}}$ (9.11), the tiny amplitudes $\Delta_M^{\mathbf{k}} \ll \mathcal{O}(1)$ of unstable superhorizon sized modes can get amplified. When they reenter the horizon after the recombination, these modes of pair-density perturbations can be of the order of unity $\Delta_M^{\mathbf{k}} \propto \mathcal{O}(1)$. As a consequence, they should have some physical influences on forming large-scale structures and galaxy cluster profiles. It would be worthwhile to study whether these Jeans-amplified pair-

density perturbations $\Delta_M^{\mathbf{k}}$ produce primordial gravitational waves when they reenter the horizon.

Further studies are required, and more elaborate numerical computations are needed. Nevertheless, we expect that our theoretical scenario and results will provide valuable insights into baryogenesis, dark matter particle-antiparticle asymmetry and the role of dark matter acoustic waves, as well as their impacts on the evolution and structure of the Universe. About the last point, it is worthwhile to mention the observational evidence indicating that dark matter inhomogeneities on scales beyond $\sim 100\text{Mpc}/h$ are larger than what is predicated by the theoretical ΛCDM model.

References

- [1] A. A. Starobinsky, *A new type of isotropic cosmological models without singularity*, *Phys. Lett. B* **91** (1980) 99.
- [2] A. H. Guth, *The inflationary universe: A possible solution to the horizon and flatness problems*, *Phys. Rev. D* **23** (1981) 347.
- [3] A. D. Linde, *A new inflationary universe scenario: A possible solution of the horizon, flatness, homogeneity, isotropy and primordial monopole problems*, *Phys. Lett. B* **108** (1982) 389–393.
- [4] V. F. Mukhanov and G. V. Chibisov, *The vacuum energy and large scale structure of the universe*, *Sov. Phys. JETP* **56** (1982) 258–265.
- [5] A. Albrecht and P. J. Steinhardt, *Cosmology for grand unified theories with radiatively induced symmetry breaking*, *Phys. Rev. Lett.* **48** (1982) 1220.
- [6] A. D. Linde, *Chaotic inflation*, *Phys. Lett. B* **129** (1983) 177.
- [7] R. Kallosh and A. Linde, *BICEP/Keck and cosmological attractors*, *JCAP* **12** (2021) 008 [[2110.10902](#)].
- [8] L. Kofman, A. D. Linde and A. A. Starobinsky, *Reheating after inflation*, *Phys. Rev. Lett.* **73** (1994) 3195 [[hep-th/9405187](#)].
- [9] L. Kofman, A. D. Linde and A. A. Starobinsky, *Towards the theory of reheating after inflation*, *Phys. Rev. D* **56** (1997) 3258 [[hep-ph/9704452](#)].
- [10] Y. Shtanov, J. H. Traschen and R. H. Brandenberger, *Universe reheating after inflation*, *Phys. Rev. D* **51** (1995) 5438 [[hep-ph/9407247](#)].
- [11] B. A. Bassett and S. Liberati, *Geometric reheating after inflation*, *Phys. Rev. D* **58** (1998) 021302 [[hep-ph/9709417](#)].
- [12] S. Tsujikawa, K.-i. Maeda and T. Torii, *Resonant particle production with nonminimally coupled scalar fields in preheating after inflation*, *Phys. Rev. D* **60** (1999) 063515 [[hep-ph/9901306](#)].

- [13] D. I. Podolsky and A. A. Starobinsky, *Chaotic reheating*, *Grav. Cosmol. Suppl.* **8N1** (2002) 13 [[astro-ph/0204327](#)].
- [14] R. Allahverdi, R. Brandenberger, F.-Y. Cyr-Racine and A. Mazumdar, *Reheating in inflationary cosmology: Theory and applications*, *Ann. Rev. Nucl. Part. Sci.* **60** (2010) 27 [[1001.2600](#)].
- [15] M. A. Amin, R. Easther, H. Finkel, R. Flauger and M. P. Hertzberg, *Oscillons after inflation*, *Phys. Rev. Lett.* **108** (2012) 241302 [[1106.3335](#)].
- [16] M. A. Amin, M. P. Hertzberg, D. I. Kaiser and J. Karouby, *Nonperturbative dynamics of reheating after inflation: A review*, *Int. J. Mod. Phys. D* **24** (2014) 1530003 [[1410.3808](#)].
- [17] P. Adshead, J. T. Giblin, M. Pieroni and Z. J. Weiner, *Constraining axion inflation with gravitational waves across 29 decades in frequency*, *Phys. Rev. Lett.* **124** (2020) 171301 [[1909.12843](#)].
- [18] L. Parker and S. A. Fulling, *Quantized matter fields and the avoidance of singularities in general relativity*, *Phys. Rev. D* **7** (1973) 2357.
- [19] A. A. Starobinsky, *Nonsingular model of the universe with the quantum-gravitational de sitter stage and its observational consequences*, *Proc. of the Second Seminar “Quantum Theory of Gravity”, Moscow, October 1981, INR Press, Moscow* (1982) 58.
- [20] L. H. Ford, *Gravitational particle creation and inflation*, *Phys. Rev. D* **35** (1987) 2955.
- [21] E. W. Kolb, A. D. Linde and A. Riotto, *Gut baryogenesis after preheating*, *Phys. Rev. Lett.* **77** (1996) 4290 [[hep-ph/9606260](#)].
- [22] D. J. H. Chung, P. Crotty, E. W. Kolb and A. Riotto, *On the gravitational production of superheavy dark matter*, *Phys. Rev. D* **64** (2001) 043503 [[hep-ph/0104100](#)].
- [23] D. J. H. Chung, E. W. Kolb, A. Riotto and I. I. Tkachev, *Probing Planckian physics: Resonant production of particles during inflation and features in the primordial power spectrum*, *Phys. Rev. D* **62** (2000) 043508 [[hep-ph/9910437](#)].
- [24] D. J. H. Chung, *Classical inflation field induced creation of superheavy dark matter*, *Phys. Rev. D* **67** (2003) 083514 [[hep-ph/9809489](#)].
- [25] D. J. H. Chung, E. W. Kolb, A. Riotto and L. Senatore, *Isocurvature constraints on gravitationally produced superheavy dark matter*, *Phys. Rev. D* **72** (2005) 023511 [[astro-ph/0411468](#)].
- [26] D. J. H. Chung, E. W. Kolb and A. J. Long, *Gravitational production of super-Hubble-mass particles: an analytic approach*, *JHEP* **01** (2019) 189 [[1812.00211](#)].
- [27] PLANCK collaboration, *Planck 2015 results. xiii. cosmological parameters*, *Astron. Astrophys.* **594** (2016) A13 [[1502.01589](#)].

- [28] A. D. Sakharov, *Violation of CP invariance, C asymmetry, and baryon asymmetry of the universe*, *Soviet Journal of Experimental and Theoretical Physics Letters* **5** (1967) 24.
- [29] A. D. Dolgov and A. D. Linde, *Baryon asymmetry in inflationary universe*, *Phys. Lett. B* **116** (1982) 329.
- [30] L. F. Abbott, E. Farhi and M. B. Wise, *Particle production in the new inflationary cosmology*, *Phys. Lett. B* **117** (1982) 29.
- [31] V. A. Kuzmin, V. A. Rubakov and M. E. Shaposhnikov, *On the anomalous electroweak baryon number nonconservation in the early universe*, *Phys. Lett. B* **155** (1985) 36.
- [32] M. Dine and A. Kusenko, *The origin of the matter-antimatter asymmetry*, *Rev. Mod. Phys.* **76** (2003) 1 [[hep-ph/0303065](#)].
- [33] M. Trodden, *Electroweak baryogenesis*, *Reviews of Modern Physics* **71** (1999) 1463–1500.
- [34] D. E. Morrissey and M. J. Ramsey-Musolf, *Electroweak baryogenesis*, *New Journal of Physics* **14** (2012) 125003.
- [35] A. Dolgov and K. Freese, *Calculation of particle production by Nambu goldstone bosons with application to inflation reheating and baryogenesis*, *Phys. Rev. D* **51** (1995) 2693 [[hep-ph/9410346](#)].
- [36] A. Dolgov, K. Freese, R. Rangarajan and M. Srednicki, *Baryogenesis during reheating in natural inflation and comments on spontaneous baryogenesis*, *Phys. Rev. D* **56** (1997) 6155 [[hep-ph/9610405](#)].
- [37] J. Garcia-Bellido, D. Y. Grigoriev, A. Kusenko and M. E. Shaposhnikov, *Nonequilibrium electroweak baryogenesis from preheating after inflation*, *Phys. Rev. D* **60** (1999) 123504 [[hep-ph/9902449](#)].
- [38] S. Davidson, M. Losada and A. Riotto, *A new perspective on baryogenesis*, *Phys. Rev. Lett.* **84** (2000) 4284 [[hep-ph/0001301](#)].
- [39] A. Megevand, *Effect of reheating on electroweak baryogenesis*, *Phys. Rev. D* **64** (2001) 027303 [[hep-ph/0011019](#)].
- [40] A. Tranberg and J. Smit, *Baryon asymmetry from electroweak tachyonic preheating*, *JHEP* **11** (2003) 016 [[hep-ph/0310342](#)].
- [41] A. Tranberg and J. Smit, *Simulations of cold electroweak baryogenesis: Dependence on Higgs mass and strength of CP-violation*, *JHEP* **08** (2006) 012 [[hep-ph/0604263](#)].
- [42] M. P. Hertzberg and J. Karouby, *Generating the observed baryon asymmetry from the inflaton field*, *Phys. Rev. D* **89** (2014) 063523 [[1309.0010](#)].
- [43] M. P. Hertzberg and J. Karouby, *Baryogenesis from the inflaton field*, *Phys. Lett. B* **737** (2014) 34 [[1309.0007](#)].

- [44] M. P. Hertzberg, J. Karouby, W. G. Spitzer, J. C. Becerra and L. Li, *Theory of self-resonance after inflation. ii. quantum mechanics and particle-antiparticle asymmetry*, *Phys. Rev. D* **90** (2014) 123529 [[1408.1398](#)].
- [45] K. D. Lozanov and M. A. Amin, *End of inflation, oscillons, and matter-antimatter asymmetry*, *Phys. Rev. D* **90** (2014) 083528 [[1408.1811](#)].
- [46] K. M. Zurek, *Asymmetric dark matter: Theories, signatures, and constraints*, *Phys. Rept.* **537** (2014) 91 [[1308.0338](#)].
- [47] S.-S. Xue, *Massive particle pair production and oscillation in Friedman universe: its effect on inflation*, *Eur. Phys. J. C* **83** (2023) 36 [[2112.09661](#)].
- [48] S.-S. Xue, *Massive particle pair production and oscillation in Friedman universe: reheating energy and entropy, and cold dark matter*, *Eur. Phys. J. C* **83** (2023) 355 [[2006.15622](#)].
- [49] S.-S. Xue, *Holographic massive plasma state in Friedman universe: cosmological fine-tuning and coincidence problems*, *JCAP* 05(2024)113 [[2309.15488](#)].
- [50] S.-S. Xue, *How universe evolves with cosmological and gravitational constants*, *Nucl. Phys. B* **897** (2015) 326 [[1410.6152](#)].
- [51] Y. Kluger, J. M. Eisenberg, B. Svetitsky, F. Cooper and E. Mottola, *Pair production in a strong electric field*, *Phys. Rev. Lett.* **67** (1991) 2427.
- [52] R. Ruffini, L. Vitagliano and S.-S. Xue, *On plasma oscillations in strong electric fields*, *Physics Letters B* **559** (2003) 12–19.
- [53] R. Ruffini, G. Vereshchagin and S.-S. Xue, *Electron–positron pairs in physics and astrophysics: From heavy nuclei to black holes*, *Physics Reports* **487** (2010) 1–140.
- [54] Q. Wang and W. G. Unruh, *Vacuum fluctuation, microcyclic universes, and the cosmological constant problem*, *Phys. Rev. D* **102** (2020) 023537 [[1904.08599](#)].
- [55] Q. Wang, *Reformulation of the cosmological constant problem*, *Phys. Rev. Lett.* **125** (2020) 051301 [[1904.09566](#)].
- [56] S.-S. Xue, *Cosmological constant, matter, cosmic inflation and coincidence*, *Mod. Phys. Lett. A* **35** (2020) 2050123 [[2004.10859](#)].
- [57] S.-S. Xue, *Cosmological Λ driven inflation and produced massive particles*, [1910.03938](#).
- [58] E. W. Kolb and M. S. Turner, *The Early Universe*, vol. 69. Westview press, A member of the Perseus Books Group, 1990, [10.1201/9780429492860](#).
- [59] B. W. Lee and S. Weinberg, *Cosmological lower bound on heavy neutrino masses*, *Phys. Rev. Lett.* **39** (1977) 165.

- [60] R. Ruffini, J. D. Salmonson, J. R. Wilson and S. S. Xue, *On the pair electromagnetic pulse of a black hole with electromagnetic structure*, *Astron. Astrophys* **350** (1999) 334 [[astro-ph/9907030](#)].
- [61] R. Ruffini, J. D. Salmonson, J. R. Wilson and S. S. Xue, *On the evolution of the pair-electromagnetic pulse of a charged black hole*, *Astron. Astrophys* **138**, 511-512 (1999) **138** (1999) 511 [[astro-ph/9905021](#)].
- [62] R. Ruffini, J. D. Salmonson, J. R. Wilson and S. S. Xue, *On the pair-electromagnetic pulse from an electromagnetic black hole surrounded by a baryonic remnant*, *Astron. Astrophys* **359** (2000) 855 [[astro-ph/0004257](#)].
- [63] J. J. Sakurai and J. Napolitano, *Modern quantum mechanics*. Cambridge: Cambridge University Press, 3rd revised edition ed., 2020, [10.1017/9781108587280](#).
- [64] L. Landau and E. Lifshiz, *Quantum Mechanics (Non-relativistic Theory)*. Elsevier Butterworth-Heinemann, 1977.
- [65] S. Hollands and R. M. Wald, *An alternative to inflation*, *Gen. Rel. Grav.* **34** (2002) 2043 [[gr-qc/0205058](#)].
- [66] J. Mielczarek, *Reheating temperature from the CMB*, *Phys. Rev. D* **83** (2011) 023502 [[1009.2359](#)].